

# Project Argonaut: A Proposal for a Mars Sample Return Mission \*

Archit Arora, Courtney Best, Liam Durbin, Robert Groome, Duncan Harris,  
Henry Heim, Thomas Keane, Eric Miller, Annie Ping, and Alexandra Wyatt

*Purdue University, West Lafayette, Indiana, 47906, United States*

With increasing interest in colonizing Mars, multiple missions have been aimed at retrieving more information about the red planet, such as the recent Mars Science Laboratory mission. The main focus of this interest is in determining whether Mars is capable of supporting life, which requires an analysis of the soil. The next major step in Martian science is a Mars Sample Return mission, which would allow scientists to conduct complicated and in-depth tests on the soil that are not possible with robotic instruments sent to Mars. This paper explores Project Argonaut, a mission proposal to retrieve a sample from the surface of Mars and bring it back to Earth. The name Argonaut reflects the legend of the band of heroes who sailed on the Argo to fetch the golden fleece from the field of Ares, as the mission requires a journey to Mars in order to retrieve the prized sample. Project Argonaut integrates existing research with innovative concepts to propose a plausible solution to the key issues associated with the mission.

---

\*Copyright © 2016 by Archit Arora, Courtney Best, Liam Durbin, Robert Groome, Duncan Harris, Henry Heim, Thomas Keane, Eric Miller, Annie Ping, and Alexandra Wyatt. Published by the American Institute of Aeronautics and Astronautics, Inc, with permission.

# Contents

<b>I</b>	<b>Introduction</b>	<b>6</b>
A	Mission Objective . . . . .	6
B	Mission Requirements . . . . .	6
C	Operation Conceptualization . . . . .	7
<b>II</b>	<b>System Dynamics</b>	<b>8</b>
A	Preliminary Analysis . . . . .	8
B	Detailed Trade Studies . . . . .	8
1	Chemical Trans-Earth Injection . . . . .	9
2	Electric Trans-Earth Injection . . . . .	10
3	Summary of Results . . . . .	11
<b>III</b>	<b>Interplanetary Transfer Vehicle (ITV)</b>	<b>11</b>
A	Propulsion . . . . .	12
1	Propulsion Requirements . . . . .	12
2	Chemical Engines . . . . .	12
3	Nuclear Engines . . . . .	13
4	Ion Engines . . . . .	13
5	Engine Selection . . . . .	14
6	Downrated HiPEP Specifications . . . . .	14
7	Attitude Control . . . . .	15
B	Structures . . . . .	16
1	General Design . . . . .	16
2	Sizing . . . . .	16
3	Material . . . . .	17
4	Mass Breakdown . . . . .	17
C	Thermal . . . . .	18
1	Passive Thermal Control . . . . .	18
2	Active Thermal Control . . . . .	18
D	Power . . . . .	18
1	Power Source . . . . .	18
2	Batteries . . . . .	19
3	Distribution and Regulation . . . . .	19
<b>IV</b>	<b>Mars Descent Vehicle (MDV)</b>	<b>19</b>
A	Systems Considered . . . . .	20
B	Design Decision . . . . .	21
C	Structures . . . . .	22
1	Parachute . . . . .	22
2	Backshell System . . . . .	22
3	Sky Crane Design . . . . .	23
4	Payload Bay . . . . .	23
5	Inflatable Heat Shield . . . . .	23
D	Navigation . . . . .	24
1	Background . . . . .	24
2	Numerical Model . . . . .	24
3	Simulations . . . . .	25
4	Results . . . . .	28
E	Entry, Descent, and Landing Description . . . . .	28
<b>V</b>	<b>Mars Ascent Vehicle (MAV)</b>	<b>28</b>
A	Propulsion . . . . .	29
1	Liquid Propellants . . . . .	29
2	Solid Propellants . . . . .	30

3	Gel Propellants . . . . .	30
4	Combination Solid and Liquid Propellants . . . . .	30
5	Hybrid Propellants . . . . .	30
6	Number of Stages . . . . .	31
7	Design Decision . . . . .	31
8	Attitude Control System . . . . .	32
B	Structures . . . . .	32
C	Thermal . . . . .	33
D	Power . . . . .	34
<b>VI</b>	<b>Earth Re-entry Vehicle</b>	<b>34</b>
A	Recovery . . . . .	35
B	Contamination . . . . .	35
C	Vehicle Design . . . . .	35
<b>VII</b>	<b>Radiation</b>	<b>36</b>
<b>VIII</b>	<b>Communications</b>	<b>36</b>
<b>IX</b>	<b>Mission Process</b>	<b>37</b>
A	Launch . . . . .	37
1	Launch Vehicle Selection . . . . .	37
2	Effects on Mission Systems . . . . .	38
B	Sample Transfer and Rendezvous . . . . .	38
1	Preliminary Analysis . . . . .	38
2	Detailed Design . . . . .	38
3	Hardware . . . . .	39
<b>X</b>	<b>Vehicle Health Monitoring and Contingency Planning</b>	<b>40</b>
A	Vital Systems Analysis . . . . .	40
B	System Monitoring . . . . .	41
C	Failure Modes . . . . .	41
<b>XI</b>	<b>Cost</b>	<b>42</b>
A	Cost Estimation Methods . . . . .	42
B	Results . . . . .	42
<b>XII</b>	<b>Conclusion</b>	<b>43</b>

## List of Figures

1	CAD model of Project Argonaut MSRS. . . . .	6
2	Relationships between customer requirements and technical requirements. . . . .	7
3	Relationships between technical requirements. . . . .	7
4	Trans-Mars injection porkchop plot. . . . .	9
5	Mars transfer orbit. . . . .	9
6	Trans-Earth injection porkchop plot. . . . .	9
7	Earth transfer orbit. . . . .	10
8	Electric Mars escape and Earth transfer. . . . .	10
9	CAD Model of the ITV. . . . .	11
10	Total propellant and engine mass of chemical engines with varying dry masses. . . . .	13
11	Propellant mass for the ion engines with different dry masses. . . . .	14
12	HiPEP engine thrust as a function of input power. <sup>9</sup> . . . . .	15
13	CAD model of ITV with outer ITV shell transparent to show inner spaces. . . . .	16
14	CAD model of MDV. . . . .	20
15	CAD model of MDV. . . . .	22
16	Top and side view of backshell. . . . .	23
17	Concept Design of HIAD. . . . .	24
18	Mass estimates for 9 diameter HIAD system. . . . .	24
19	Results of unguided test. . . . .	26
20	Guided flight paths for target of 1800 km downrange. . . . .	26
21	Illustration of the MDV miss distances. . . . .	26
22	Entry trajectory for low flight angles. . . . .	27
23	MDV target ellipse with hazard. . . . .	27
24	Isometric view of MAV. . . . .	29
25	Isometric view of MAV interior with labels. . . . .	33
26	Cross section of MAV. . . . .	34
27	Isographic and side views of the ERV CAD. . . . .	34
28	CAD of ERV sample holding system. . . . .	35
29	Views of the ITV CAD model with solar panels deployed and retracted. . . . .	44
30	Side view of MSRS assembly. . . . .	44
31	Technical dimensions of ERV model. . . . .	44
32	Technical dimensions of ITV model. . . . .	44
33	Technical dimensions of MDV model. . . . .	45
34	Technical dimensions of MAV model. . . . .	45

## List of Tables

1	Mission requirements analysis as set by the RFP. . . . .	6
2	Trans-Mars injection characteristics. . . . .	9
3	Trans-Earth injection characteristics. . . . .	10
4	Electric Trans-Earth injection characteristics. . . . .	10
5	System analysis summary. . . . .	11
6	List of technical requirements and their effects on each system. . . . .	12
7	Mass estimates for chemical engines with 10,000 kg dry mass. . . . .	13
8	Total mass of propellant and engine with ion engines with estimated dry mass of 10,000kg. . . . .	14
9	Mass distribution between RL-10B-2 and HiPEP. . . . .	14
10	Chosen downrated HiPEP specifications. <sup>11</sup> . . . . .	15
11	Mass distribution for the downrated HiPEP engine. . . . .	15
12	Mass distribution for the downrated HiPEP engine. . . . .	17
13	Mass breakdown for the ITV. . . . .	17
14	Comparison of Ultraflex and SLASR solar arrays. . . . .	19
15	List of technical requirements for the MDV. . . . .	20
16	Descent method decision matrix. . . . .	21
17	Total mass breakdown for MDV. . . . .	22

18	List of dimensions based off of MSL Parachute system. <sup>30</sup>	23
19	Summary of model initial inputs.	25
20	Summary of scenario results.	27
21	List of technical requirements for the MAV.	29
22	Comparison of selected MAV propulsion systems. <sup>43,50</sup>	32
23	Volumes of propellants in MAV model.	32
24	Launch vehicle requirements and constraints.	34
25	Launch vehicle requirements and constraints.	37
26	Summary of the requirements for rendezvous.	38
27	Possible rendezvous profile configurations.	38
28	Summary of ITV rendezvous operations.	39
29	Vital mission components and associated health factors.	40
30	Health factors and associated mechanism for measurement and monitoring.	41
31	Cost comparison from different organizations. <sup>79-82</sup>	43
32	Power requirement breakdown by system.	46
33	Mass requirement breakdown by system.	46
34	Morphological chart of all design solutions.	47

## Nomenclature

<i>ACS</i>	Attitude Control System	<i>MLI</i>	Multi-Layer Insulation
<i>AMCM</i>	Advanced Method Cost Model	<i>MRO</i>	Mars Reconnaissance Orbiter
<i>AR&amp;C</i>	Automate Rendezvous and Capture	<i>MSL</i>	Mars Science Laboratory
<i>ATC</i>	Active Thermal Control	<i>MSR</i>	Mars Sample Return mission
<i>AVGS</i>	Advanced Video Guidance System	<i>MSRS</i>	Mars Sample Return System
$C_3$	Characteristic Energy	<i>OE</i>	Orbital Express
<i>CER</i>	Cost Estimate Relation	<i>O/F</i>	Oxidizer to fuel ratio
<i>DET</i>	Direct Energy Transfer	<i>OpNav</i>	Optical Navigation
<i>EDL</i>	Entry Descent and Landing	<i>OS</i>	Orbital Sample
<i>ERV</i>	Earth Re-entry Vehicle	<i>PPT</i>	Peak Power Tracker
<i>GN&amp;C</i>	Guidance Navigation and Control	<i>RCS</i>	Reaction Control System
$\Delta H$	Difference in semi-major axis altitudes	<i>RFP</i>	Request for Proposal
<i>HiPEP</i>	High Power Electric Propulsion Engine	<i>RTG</i>	Radioisotope Thermoelectric Generator
$I_{sp}$	Specific Impulse	<i>SLASR</i>	Stretched Lens Array Square Rigger
<i>ISS</i>	International Space Station	<i>SOR</i>	Stable Orbit Rendezvous
<i>ITV</i>	Interplanetary Transfer Vehicle	<i>TMI</i>	Trans-Mars Injection
<i>LEO</i>	Low Earth Orbit	<i>TRL</i>	Technology Readiness Level
<i>L/D</i>	Lift to Drag Ratio	<i>UHF</i>	Ultra High Frequency
<i>LiDAR</i>	Light Detection and Ranging	$\Delta V$	Change in Velocity
<i>MAV</i>	Mars Ascent Vehicle	<i>VNS</i>	Visual Navigation System
<i>MDV</i>	Mars Descent Vehicle		

# I. Introduction

## A. Mission Objective

The objective of the Mars Sample Return (MSR) mission is to design an unmanned Interplanetary Transfer Vehicle (ITV) capable of retrieving a sample cache from a rover on Mars. The ITV will transport the Mars Descent Vehicle (MDV) to land on the surface within an acceptable range of the Mars 2020 rover, the Mars Ascent Vehicle (MAV) to launch the sample cache into orbit, and the Earth Reentry Vehicle (ERV) to protect the sample on the return trip.

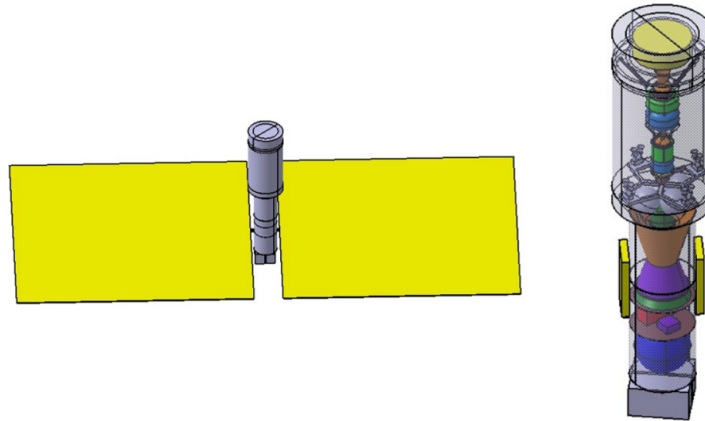


Figure 1. CAD model of Project Argonaut MSRS.

## B. Mission Requirements

To establish the most important specifications of the Mars Sample Return System (MSRS), as well as the relationships between these specifications, a house of quality was generated. This provided a guideline for the criteria that the mission must meet and the constraints within which the mission design must operate. The Request for Proposal (RFP) outlines multiple requirements that the MSRS profile must be designed to complete. The mission must work within the distance, range, and timeline of the robotic science rover; this places constraints on certain parameters. Overall, every component of the MSRS must be feasible and reliable, with the safety of the sample as the highest priority. These requirements are described in greater detail in Table 1.

Table 1. Mission requirements analysis as set by the RFP.

Mission Requirements	Criteria	Target Values
Transport MAV to designated location	Ability to land at multiple locations on Mars	Rover location
MAV survival duration	Ability to survive on Mars for a length of time	> 50 Earth days
Work within MSRS mission timeline	Land within operable lifetime of rover	February 2023
Mars descent accuracy	Land within specified distance of rover	Within 5 km
Integration with the rover	Ability to receive sample within rover arm range	< 2 m high
Integration with the sample container	Ability to hold a payload with the volume and mass of the sample container cylinder	15 cm dia. x 15 cm long, mass of 3 kg
Mission feasibility	Sufficient Technology Readiness Level (TRL)	6 or above

Each of these requirements was given a weight based on their relative importance to the overall success of the mission. This provides a means of judging decisions that affect multiple subsystems. Meeting the



## II. System Dynamics

The singular mission purpose allows for a large pool of viable mission architectures. In order to select a feasible architecture, preliminary and detailed studies were conducted. The rover will land on Mars in February 2021 and will have an operational phase of two Earth years. As a result, any retrieval attempts must be made before this time to maximize the probability of a successful sample transfer. Different combinations of parameters yield mission architectures of varying feasibilities that can be examined in more detail.

### A. Preliminary Analysis

The number of launches was first considered. The number of launches could be increased to permit on orbit assembly of vehicles that cannot fit into a single launch vehicle. Alternatively, the number of launches could be increased to split the mission into various components, which would allow risk to be spread among various missions. However, separating into multiple launches increases the cost and complexity, as additional launch dates and trajectories would have to be determined. Additionally, using multiple launches to assemble the ITV in Low Earth Orbit (LEO) was considered for cost savings. However, given the relatively low final mass of the ITV, a single launch proved more efficient, cost effective, and less complex.

The considered propulsion systems, chemical propulsion and solar electric propulsion (SEP), both have very distinct trajectories. Chemical propulsion allows for a less complicated trajectory design and optimization, simplifying the design process and flight operations. However, chemical engines typically have a much lower specific impulse ( $I_{sp}$ ), requiring larger propellant masses. With SEP, more maneuvers can be conducted without a major impact on the ITV mass. This would allow the ITV better maneuverability for accurate MDV deployment. However, the low thrust provided by SEP requires that any maneuvers occur over a relatively long period of time. If SEP was used for the Trans-Earth Injection, the ITV would be exposed to radiation from the Van Allen Belt and orbital debris for a prolonged period of time. This introduces additional requirements on the attitude control system (ACS). Additionally, long burn times increase the demands on the engine reliability, which have an inherent risk of failure during a maneuver.

Upon arrival at Mars, there are two options for orbital insertion: powered deceleration and aerocapture. Depending on a retro burn for insertion requires a chemical engine to impart a large enough thrust for timely deceleration. This necessitates chemical propulsion, or a combination of chemical and electric. Either configuration would greatly increase the propellant mass and therefore the cost. In contrast, aerocapture requires a heat shield and thrusters for minor adjustments during the capture process.

The final mission architecture was selected based on the considerations detailed above. The optimal number of launches was determined to be one, as the reduced risk provided by multiple launches does not justify the associated increase in mission cost and complexity. Additionally, launch delays could disrupt the entire mission timeline. Due to the time constraint involved in the arrival at Mars and sample transfer, the TMI was selected to use chemical propulsion. A low thrust trajectory would take an infeasible amount of time and is therefore not viable for the transfer to Mars. However, rather than adding an additional chemical engine to the ITV, the injection maneuver could be performed by the launch vehicle, which would eliminate the need for the ITV to possess multiple propulsion systems if electric propulsion is used for the return trajectory. Modern launch vehicles are typically capable of providing a characteristic energy ( $C_3$ ) in excess of  $10 \text{ km}^2/\text{s}^2$  for vehicles of a similar mass, making such a maneuver a viable option.<sup>1</sup> For Mars insertion, the relatively high cost of a powered deceleration using a chemical engine, adding about 2436 kg of propellant, would add considerable cost. On the other hand, using a SEP for the deceleration would only add 43 kg of fuel, but extends the time of deceleration to upwards of 260 days. As a result, aerocapture was selected as the more feasible option. In order to determine the relative feasibility of the two trans-Earth injection possibilities, more detailed designs and models were defined and compared.

### B. Detailed Trade Studies

With either the chemical or SEP configurations, the MSRS will be placed directly into a TMI trajectory by the launch vehicle. The characteristics of the injection are obtained from Fig. 4. On 1/29/2021, the ITV will arrive at Mars, and an aerocapture will be performed to insert the ITV into a 500 km circular orbit. From there, the MDV is released. The MAV then launches from the Martian surface and transfers the OS to the ITV, which then departs for Earth. This trans-Earth injection can be performed by either a chemical or an electric propulsion system.



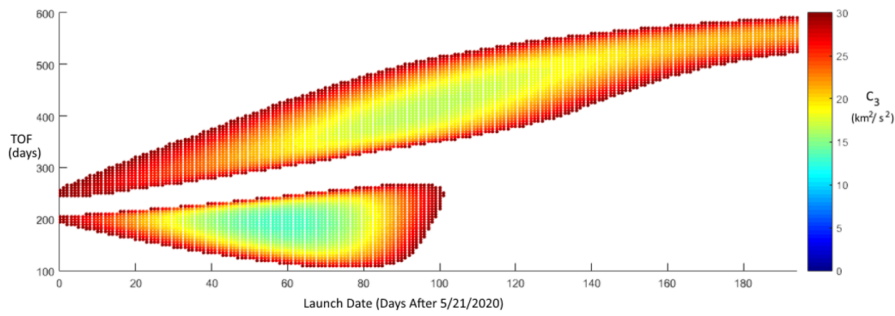


Figure 4. Trans-Mars injection porkchop plot.

Table 2. Trans-Mars injection characteristics.

Trajectory	Type I
Date	7/19/2020
$C_3$ ( $\text{km}^2/\text{s}^2$ )	13.1821
Arrival V Infinity ( $\text{km/s}$ )	2.8533
Time of Flight (days)	193

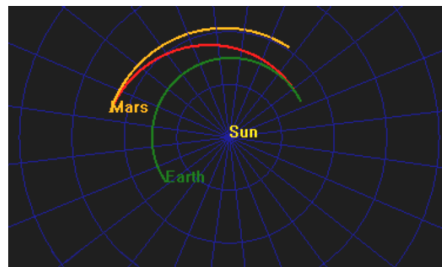


Figure 5. Mars transfer orbit.

### 1. Chemical Trans-Earth Injection

The procedure for the chemical trans-Earth injection matches that of the TMI. The porkchop plot shown in Fig. 6 is used to determine a feasible trajectory for the return to Earth. On 4/21/2023, the orbiter will reach Earth and insert into orbit via aerocapture. Then, the ERV detaches and deorbits for recovery.

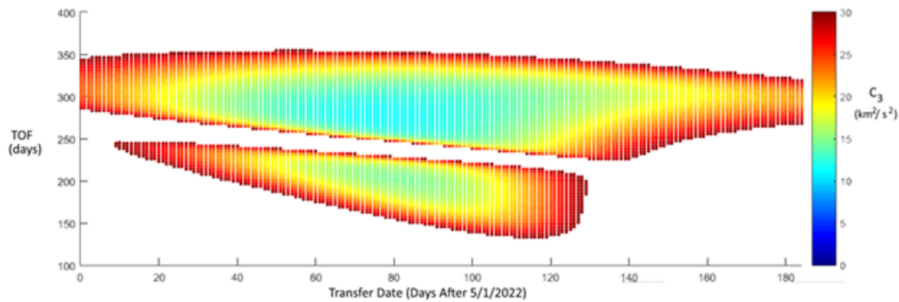
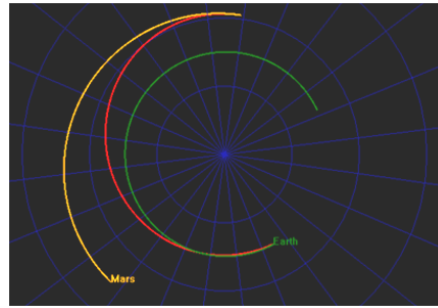


Figure 6. Trans-Earth injection porkchop plot.

**Table 3. Trans-Earth injection characteristics.**

Trajectory	Type II
Date	7/18/2022
$C_3$ (km <sup>2</sup> /s <sup>2</sup> )	11.3617
$\Delta V$ (km/s)	2.4728
Propellant Mass (kg)	2076
Payload Mass (kg)	1802.83
Arrival V Infinity (km/s)	3.2052



**Figure 7. Earth transfer orbit.**

## 2. Electric Trans-Earth Injection

Due to the path-dependent nature of low thrust trajectories, the analysis procedure for electric injection differs from chemical. The low thrust trajectory is fixed to the least optimized option. The trajectory assumes a constant thrust along the velocity direction and trajectory that transfers between the Mars aphelion and the Earth perihelion. These two assumptions provide a trajectory near the upper limit of total required impulse and is a reasonable estimate for use in a more detailed design.

**Table 4. Electric Trans-Earth injection characteristics.**

Propellant Mass (kg)	255
Payload Mass (kg)	1802.83
Time of Flight (days)	478

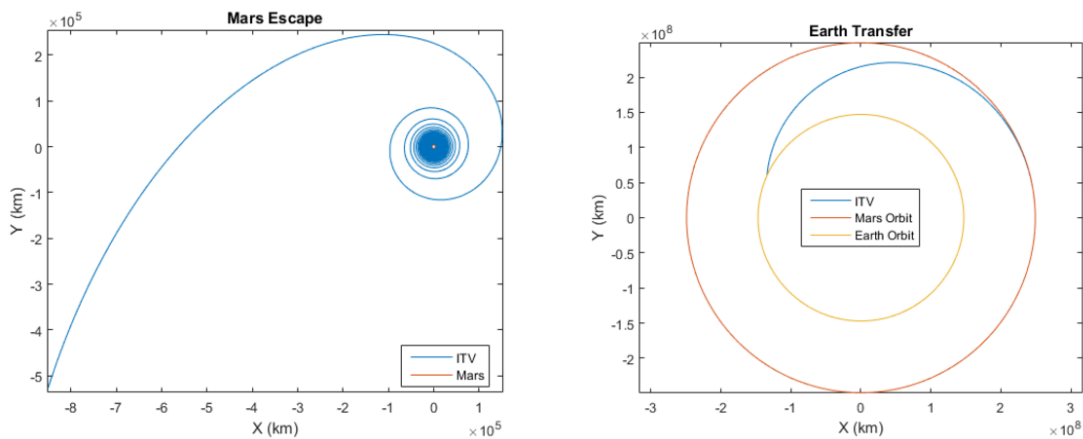


**Figure 8. Electric Mars escape and Earth transfer.**

### 3. Summary of Results

With both chemical and SEP systems analyzed, a comparison was made and a final design selected. The main parameters to be compared between the two system types are propellant mass and the time of flight, as shown in Table 5. Selecting electric propulsion over chemical propulsion reduces the propellant requirement by 88%. However, it also increases the time of flight of the return trip by 73%. The main constraint for the mission during the return trip is the cost; there is no time constraint for the return to Earth beyond radiation protection. SEP also permits the design of orbits that support access to any location on the surface. As a result, the electric propulsion was selected for further design as it greatly reduces the cost through much lower propellant requirements, while not adversely affecting mission completion with a longer time of flight.

**Table 5. System analysis summary.**

Parameter	Chemical Propulsion	Electric Propulsion
Propellant Mass (kg)	2076	255
ITV Wet Mass (kg)	3878.83	2057.83
Time of Flight (days)	277	478

During the mission, the ITV may have to change orbital inclination to achieve a suitable orbit to detach the MDV for descent. With a departure from Cape Canaveral, the ITV will have a declination of approximately  $28^\circ$  upon Mars arrival, which means that the maximum inclination change the ITV will have to conduct will be  $152^\circ$ . With a chemical engine, the propellant cost will be considerably higher, but the change in inclination will be almost instantaneous. The  $\Delta V$  to alter the inclination by  $152^\circ$  at Low Mars Orbit would be 6.439 km/s, which would have an associated propellant mass of 8528 kg. To reduce the  $\Delta V$ , the plane change maneuver could be performed during the aerobraking procedures, which would place the ITV into a highly elliptic orbit. At the apoapsis of this orbit, at approximately 450000 km, the orbital velocity would be much lower reducing the  $\Delta V$  to a more manageable 1.763 km/s. But even with this reduction in  $\Delta V$ , the ITV would still require an additional 3036 kg of propellant. On the other hand, using SEP, the propellant mass can once again be significantly reduced at the expense of TOF. To conduct a plane change in low Mars orbit, the ITV would need to conduct a  $\Delta V$  of 3.318 km/s which would take approximately 77 days to complete. This would require 86 kg of propellant.

### III. Interplanetary Transfer Vehicle (ITV)

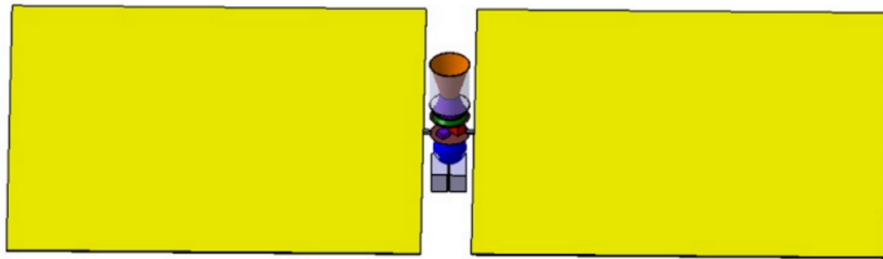


**Figure 9. CAD Model of the ITV.**

The ITV is assigned the major task of transporting all components of the MSRS. The vehicle encompasses the MDV, MAV, and ERV. As no vehicle has made a round trip from Mars, the ITV faces some technological challenges in each system that will be discussed in their respective sections. The design of the ITV was carefully constructed based on the requirements listed in Table 6.

**Table 6. List of technical requirements and their effects on each system.**

Technical Requirements	Affected Systems
Mass under 130,000 kg (max payload mass for SLS)	All Vehicle Systems
Fit within dimensions of launch system	Structural Design, Propulsion System
Capable of roundtrip to Mars	Propulsion System, Power System, Radiation System
Contain the MDV, MAV, and ERV	Structural Design
TRL of 6 or above	All Vehicle Systems

## A. Propulsion

Multiple propulsion systems have been developed that fit the requirements of this mission. The propulsion system chosen will contain a main engine, as well as smaller thrusters for corrections in the trajectory and altitude control. The system must be efficient, powerful, and last the duration of the mission. The main engine has to provide enough thrust to compensate for the additional velocity necessary for changes in trajectory throughout the mission. The engine types considered were chemical, ion, and nuclear, with further research and analysis done on each to determine the appropriate engine for the mission.

### 1. Propulsion Requirements

The  $\Delta V$  requirements for the mission depend primarily on the engine type. The engine has to provide enough thrust to reach the  $\Delta V$  of each burn within the burn time of the engine. For chemical engines, the first burn requires a  $\Delta V$  of 3.8 km/s. If the engine can produce the thrust necessary for the  $\Delta V$  of the first burn, it can provide the thrust required for the other smaller  $\Delta V$  burns. For ion engines, the thrust is relatively small and will accumulate over time to reach the  $\Delta V$  required. Multiple engines can be used to accommodate for the low thrust; however, mass will be increased with every additional engine.

The mass and size of the propulsion system, which includes the engine(s), propellant, and propellant tank(s), are to be minimized to reduce cost. Therefore, engines with high thrust-to-weight ratios were considered. Since a majority of the mass of the ITV will be propellant, an efficient engine is desired to minimize the propellant mass and volume. A smaller volume equates to smaller tanks and less insulation, lowering the mass of the entire ITV. A smaller volume will decrease the number of launches needed and allow the ITV to launch within a smaller vehicle. The constraints on the sizing will affect the design of the propellant tank(s) and the arrangement of the engine(s). The design of the propulsion system has to meet the constraints of the launch system chosen while also accommodating the needed propellant volume.

### 2. Chemical Engines

Chemical rocket engines are by far the most proven and most commonly used type of spacecraft propulsion in the industry. However, chemical engines are very inefficient. Chemical rockets have fuel efficiencies up to 35%, while ion engines can have efficiencies of over 90%.<sup>2</sup> All previous missions to Mars have used chemical engines for interplanetary travel, but as the payload mass and travel distance increases, a more efficient engine is needed. Many different existing chemical engines were researched to see if any could fulfill the mission requirements. The five top performing contenders are shown in Table 7 with propellant and engine mass calculations for a hypothetical 10,000 kg dry mass. All of the engines shown except for the Merlin 1-D use a combination of liquid hydrogen and liquid oxygen for propellant. The Merlin 1-D uses RP-1, or rocket grade kerosene, and liquid oxygen. The two Aerojet Rocketdyne RL-10 engines and the SpaceX Merlin engine are currently in use for launch vehicles and have proven themselves as capable and reliable. The development and testing of the J-2X was put on hold in 2014 due to low funding.<sup>3</sup> The RL-60 was being developed by Aerojet Rocketdyne as a replacement for the RL-10 series, but has been shelved after successful testing. It can be seen that the propellant masses are all over forty times larger by mass than the propellant mass using an ion engine. From Fig. 10, although the RL-60 engine is the best chemical engine to use for the mission due to the low total propellant and engine mass, its lack of development makes the RL-10B-2 engine the best option from the list of chemical engines for further analysis.

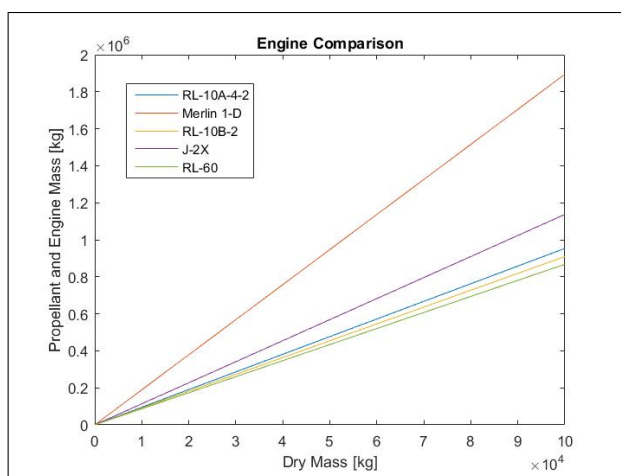


Figure 10. Total propellant and engine mass of chemical engines with varying dry masses.

Table 7. Mass estimates for chemical engines with 10,000 kg dry mass.

Engines	RL-10A-4-2	RL-10B-2	Merlin 1-D	J-2X	RL-60
Propellant Mass (kg)	64,546	61,597	115,490	65,379	59,609
Engine Mass (kg)	167	277	470	2,430	499
Number of Engines	3	3	1	1	1
Total System Mass (kg)	65,047	62,428	115,960	67,827	60,108

### 3. Nuclear Engines

Nuclear thermal engines typically have an  $I_{sp}$  and thrust between ion and chemical engines.<sup>5</sup> In this way, nuclear engines are a middle ground between the two methods, and could be suitable for this mission. However, if the launch vehicle for this mission failed on ascent with nuclear material on board, there is a chance that that material could contaminate the surroundings. Also, nuclear thermal engines require a large volume of fuel, because the most efficient propellant, hydrogen, has a low density.<sup>4</sup> Finally, the nuclear thermal engines themselves are very heavy due to the thick shielding required to prevent radiation from escaping containment. NERVA, a nuclear thermal propulsion project developed by NASA, was projected to have a mass of 10,400 kg.<sup>5</sup>

### 4. Ion Engines

Ion engines are safer than chemical engines and ten times more efficient. The high efficiency is achieved by providing high velocity exhaust while minimizing the mass flow rate, which reduces the amount of propellant required for the entire mission. This will decrease the size and cost off the ITV considerably.<sup>6</sup> The downside of ion propulsion is the time needed to generate sufficient thrust, because it is accumulated over a long period of time.<sup>7</sup> The NASA Dawn spacecraft used the NASA Solar Technology Application Readiness program ion thruster for its main engine. Dawn reached Mars in a year and a half during its mission, which validates the use of the engine for the MSRS.<sup>8</sup> NASA has also developed a new ion engine named the High Power Electric Propulsion engine (HiPEP), which is more efficient and powerful than the Dawn engine. There are multiple downrated versions of the HiPEP that are not as efficient but will require less power, which were also considered.<sup>9</sup> Analysis was also done on the ion engines used on the two all-electric satellites by Boeing, which are the least efficient of the studied engines as seen in Fig. 11.<sup>10</sup> Table 8 shows the propellant mass and engine mass for the ion engines with a hypothetical dry mass of 10,000 kg.

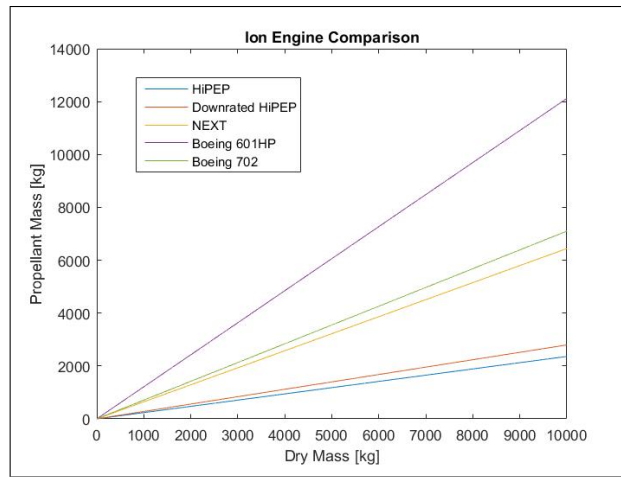


Figure 11. Propellant mass for the ion engines with different dry masses.

Table 8. Total mass of propellant and engine with ion engines with estimated dry mass of 10,000kg.

Engines	HiPEP	Downrated HiPEP	NEXT
Propellant (kg)	1723	2031	4520
Engine Mass (kg)	443	443	58.2
Total System Mass (kg)	2166	2474	4578

### 5. Engine Selection

After further analysis and proper sizing of the ITV, the ion engine was ultimately selected as the main engine for the mission due to the required propellant mass shown in Table 9. Calculations were made assuming a payload mass of 800 kg for the MAV, MDV, and the ERV. The total mass for the RL-10B-2 is over the mass limit of any existing launch vehicle, including the Space Launch System (SLS). The HiPEP engine has considerably less mass compared to the RL-10B-2 and can fit into any launch system given the total mass. The only complication with the use of the HiPEP engine is the high power consumption, which would necessitate large solar panels. The problem is solved by using a downrated HiPEP, which is not as efficient as the HiPEP but consumes less power.

Table 9. Mass distribution between RL-10B-2 and HiPEP.

Mass Distribution (kg)	RL-10B-2	HiPEP
Dry Mass	17,404	2,447
Payload Mass	800	800
Inert Mass	16,604	1,647
Propellant Mass	16,604	1,647
Total Mass	173,658	3,165

### 6. Downrated HiPEP Specifications

The main engine selected for the MSRS is the downrated HiPEP with the engine specifications in Table 10. The engine was chosen after considering the power consumption of the regular HiPEP engine. It can be seen in Fig. 12 that the thrust and the input power has a positive linear relationship. The selected downrated version provides a balance between efficiency and power consumption. Lower power consumption would decrease the size of the solar panels and the mass of the structures. However, this would increase the propellant mass required, which will null the decrease in mass from the solar panels. The primary concern was the sizing of the solar panels, since the structure must fit within a launch vehicle.

HiPEP was initially developed by the NASA Glenn Research Center for the Jupiter Icy Moons Orbiter project set for launch in 2017. The project was later canceled in 2005 due to a shift in focus towards manned missions.<sup>6</sup> The engine had a TRL of a 4 at the time of cancellation. However, based on an AIAA article written in 2009, HiPEP will be ready for use on a mission within nine years, or by 2018. The thruster has been wear-tested at 20.8 kW for 2000 hours at an  $I_{sp}$  of 7650 seconds, a thrust of 0.43 N, and an overall thruster efficiency of 77%. HiPEP also has a substantial life capability and will last the duration of the mission.<sup>12</sup> The ITV will contain two HiPEP engines; however, only one will be used at a time. The other engine will be used as a replacement in case of failure in the first engine. The thruster is rectangular in design with an approximately 41 x 91 cm ion extraction plane.

**Table 10. Chosen downrated HiPEP specifications.<sup>11</sup>**

Power (kW)	24.4
Flow Rate (mg/s)	5.6
Efficiency	0.76
Thrust (mN)	460
Specific Impulse	8270
Mass (kg)	443

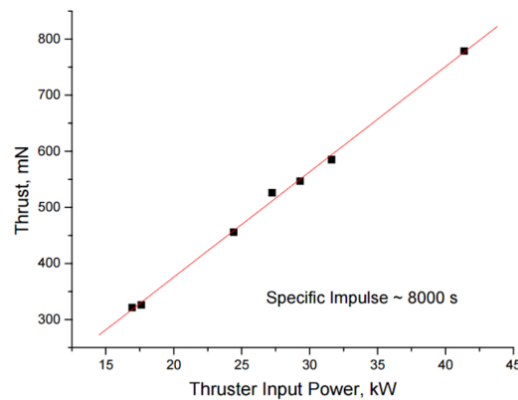


**Figure 12. HiPEP engine thrust as a function of input power.<sup>9</sup>**

The engine uses xenon gas, compressed to a density of 1500 kg/m<sup>3</sup>. The trip will require 483 kg of xenon, with a volume of 0.32 m<sup>3</sup>. The propellant mass includes a 30% contingency on the  $\Delta V$  required and accounts for a 30% design margin for the ITV structure. Table 11 shows the mass distribution after proper sizing of the ITV and finalizing the mass of the separate components.

**Table 11. Mass distribution for the downrated HiPEP engine.**

Component	Mass (kg)
Dry Mass	2529
Payload Mass	913
Inert Mass	1617
Propellant Mass	483
Hydrazine Mass	50
Total Mass	3062

## 7. Attitude Control

The ACS used on the ITV will be similar to the one used on Dawn. The HiPEP will be mounted to a two-axis gimbal. This arrangement allows for change in the center of gravity during flight and to allow the ACS

to control attitude when thrusting. During normal cruise, a star tracker will be used to estimate attitude and rates. Coarse Sun Sensors will be used for rough attitude determination and for fault protection. The ACS will control the use of the reaction control system (RCS) or the reaction wheels, depending on the situation to adjust the attitude. The RCS is hydrazine based and will be used for direct control of attitude or for desaturation of the reaction wheels. It can also be used for an additional boost in  $\Delta V$  in case there is insufficient time to reach the  $\Delta V$  required to maneuver around incoming asteroid or space debris. The RCS will have two independent strings with six thrusters each, capable of producing 0.9 N of thrust. Each string will have a pair of thrusters pointing in the +x, -x, and -z directions. The design provides a contingency in case one string malfunctions. The system requires about 50 kg of hydrazine propellant. The ACS is 37 kg and the RCS is 14 kg, making the dry mass of the entire system 51 kg.<sup>13</sup>

## B. Structures

The ITV is designed to be the central vehicle of the mission. The MAV, MDV, and ERV all begin the mission connected to the ITV. The physical design of the ITV was heavily influenced by its main objective of transporting all components of the MSRS.

### 1. General Design

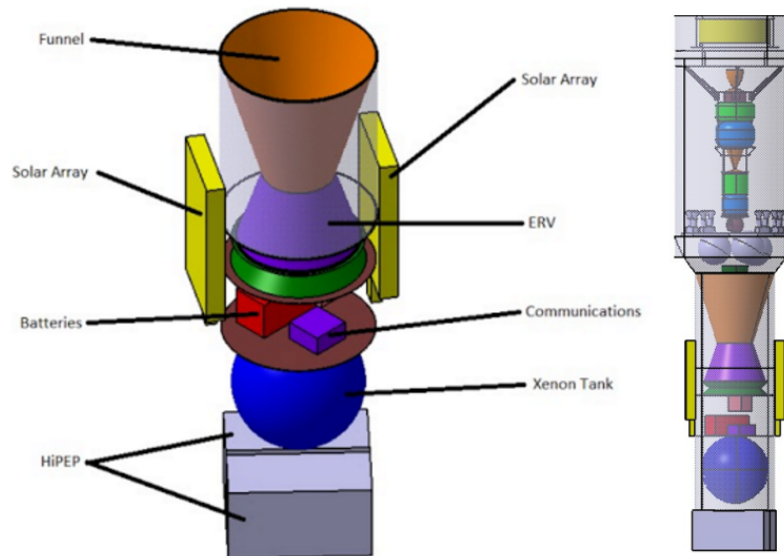


Figure 13. CAD model of ITV with outer ITV shell transparent to show inner spaces.

The ITV must fit inside a standard launch fairing and contain several key systems. The engines must be placed in line with the center of mass, and the ITV must incorporate space for the xenon propellant tanks, the ACS system, flight control and communication equipment, ERV/MDV/MAV placement, and other various systems. Taking these considerations into account, the ITV was designed to be cylindrical, with the majority of systems located inside the cylinder for protection. The xenon tank is positioned at the bottom of the cylinder near the engines. Above the xenon tank is space allocated for internal systems, including the hydrazine tanks, flight control computers, communications equipment, and gyroscopes. Above the ERV, a funnel that allows safe OS capture is affixed to the cylinder. For the reentry phase of the mission, the funnel section at the end of the ITV will be jettisoned using pyrotechnics during the return trajectory. The ERV will then be mechanically released from the ITV once it is in position near Earth. Finally, above the funnel the MDV and MAV are attached to the ITV via a decoupler.

### 2. Sizing

The tank is a sphere to maximize volume and minimize surface area, decreasing the amount of insulation required. The sphere has a diameter of 0.85 m, which provides a constraint on the minimum diameter of the ITV. The inside diameter of the ITV is 0.9 m, to allow room between the Xenon tank and the ITV



outer wall. This extra space will aid in the construction of the ITV, and gives ample room for insulation and structural support. Below the tank there is a 2 m long space allocated for other systems, which is sufficient for the navigation, communication, power, and control systems. Spaced throughout the ITV are cylindrical supports, which will provide structural stability and integrity. The ERV is positioned within the ITV cylinder with the heat shield facing the engine, in order to simplify placement of the sample container inside the ERV. The ERV is contained within a vertical space of 0.546 m between a cylindrical support and the MDV attachment mechanism, and rests on a cylindrical base of 5 mm radius bars. This base protects the heat shield from damage during launch.

### 3. Material

The ITV will undergo significant forces and temperature fluctuations during the mission; therefore a variety of building materials were considered. 6061 Aluminum is a very common alloy of aluminum, used for a wide variety of applications. 7075 Aluminum is used in many aircraft-related applications, as it is one of the strongest aluminum alloys.<sup>14</sup> R56400 Titanium is one of the strongest titanium alloys, used for vital systems such as aircraft landing gear, and low-volume spacecraft structures.<sup>15</sup> Both aluminum and titanium alloys are capable of storing cryogenic propellant in high temperatures up to 177°C and 427°C respectively, which is higher than the maximum of 150°C that will be experienced in the mission.<sup>14, 15</sup> Table 12 compares these materials, all of which are reliably used in industry and would prove simple and cost effective for manufacturing use. R56410 Titanium is the clear choice out of the listed materials, as it has the highest shear strength, tensile yield strength, and modulus of elasticity. Additionally, the titanium has by far the highest density, indicating its high strength within a low mass.

**Table 12. Mass distribution for the downrated HiPEP engine.**

Material	Density (g/cc)	Shear Strength (MPa)	Tensile Yield Strength (MPa)	Modulus of Elasticity (GPa)
6061-T6 Aluminum	2.7	207	276	68.9 [ASM1]
7075-T6 Aluminum	2.81	331	503	71.7 [ASM2]
R56400 Titanium	4.43	550	880	113.8 [ASM3]

### 4. Mass Breakdown

The mass breakdown for the ITV is shown in Table 13. The entire ITV is sized based on the propellant required for the MSRS. From the final ITV design, the mass is estimated using a combination of research and calculations using the density of the materials used in each component. The table shows the budgeting for the mission and the design margins allotted for the manufacturing phase.

**Table 13. Mass breakdown for the ITV.**

Inert Mass Breakdown (kg)	Estimates (30%)	Budgeted	Margins
Xe Tank	13	15	2
Hydrazine Tank	4	5	1
Insulation	13	15	2
Fairing	58	67	9
Engines	886	1019	133
Avionics	172	198	26
Wiring	53	62	8
Solar Panels	184	212	21
Batteries	112	129	17
Heatshield	75	86	11
Attitude Control	51	59	8

## C. Thermal

The ITV will experience temperature fluctuations throughout the mission. The main thermal loads will be from the heat generated by onboard equipment and the Sun, which can reach up to 150°C. The deviation in temperature will occur due to the shadows caused by the positioning of the ITV relative to the Sun and the planets. This shade can cause the temperature to drop to -125°C. The temperature maintained by the system is required to be within the operating temperature range of all the equipment and stable throughout the mission. The temperature should also be uniform throughout the ITV.<sup>16</sup>

### 1. Passive Thermal Control

In order to minimize power intake and cost, a passive system is considered in combination with an active system. Since sunlight is the major source of heating, the external surfaces of the ITV will experience a wide deviation of temperatures due to shadows. To mitigate the problem, a wavelength dependent thermal coating will be applied to the outer surfaces of the ITV. Black paint will be applied to the interior of the ITV to distribute the temperature within the vehicle. Additionally, multi-layer insulation (MLI) will be installed on the outer surfaces to minimize the radiative heat transfer. MLI consists of lightweight reflective films with multiple layers to reduce emittance, reflecting 95% of the radiation in the environment.<sup>16</sup> The MLI will be gold colored, which is a very efficient IR reflector.<sup>17</sup> The insulation will consist of 16 layers of Kapton, Dacron, and Mylar polyester film, resulting in an insulation thickness of 1 mm. The number of layers is based on Cassini, which contained 17 layers. Each layer contains tiny holes to prevent trapping gas within the vehicle. MLI also serves as micrometeoroid protection for any high-speed submillimeter-size particles. The same insulation system will be used for the propellant tanks as protection from heat transfer within the ITV from onboard equipment.<sup>18</sup> MLI was chosen because of its well-established flight history. Single-layer radiation barriers can also be used in places where less thermal insulation is required, because they are cheaper and lighter than the MLI. Other material options include foam, batt, and aerogel, which can be used in environments containing gas where MLI loses effectiveness.<sup>19</sup>

### 2. Active Thermal Control

The passive control system retains the temperature of the ITV in the space environment; however, it alone cannot provide sufficient thermal control, as the ITV must reject the heat retained by the MLI within the vehicle. An active thermal control (ATC) system will be used during normal operation. The system considered includes heaters, louvers, heat pipes, thermoelectric coolers, and radioisotope heating units.<sup>19</sup> The ATC will include autonomous, thermostatically controlled resistive electric heaters, as well as electric heaters that can be controlled from a base on Earth. Temperature sensors will be placed in various locations within the ITV to determine whether the temperature is within the operational temperature of the on-board equipment. Louvers will also be used to help minimize electrical power used for heaters.<sup>17</sup>

## D. Power

Electrical power systems are a critical subsystem that facilitate the function of every other subsystem. The total necessary power for the spacecraft is approximately 28 kW. The majority of that required power is needed to power the 25 kW HiPEP engine used on the ITV. The system will include a power source, batteries, and a distribution and regulation component.

### 1. Power Source

Various sources were considered to provide the necessary power to the spacecraft systems. The main sources considered were solar panels, Radioisotope Thermoelectric Generators (RTG), and fuel cells, all heritage technologies. The advantages of RTG include their low mass, compact structure, and long life. Additionally, they do not require sunlight, and are relatively insensitive to the low temperatures and high radiation of space. Some major disadvantages include that they cannot be turned off, have to be cooled and shielded, and are very expensive. The projected cost for the 28 kW power system using a linear fit based on three types of RTG is \$4.2 billion, and the projected mass for that system is over 8300 kg, more than double the ITV mass.<sup>20</sup> The space shuttles used three fuel cell units, which produced 21 kW continuously, using hydrogen and oxygen.<sup>21</sup> Some advantages of fuel cells are that they have a high specific power and a reversible reaction,

making regenerative fuel cells possible. However, they are generally only feasible for shorter missions in the range of days rather than years. Solar panels have a long heritage, high reliability, high specific power, and low specific cost. However, they experience a deterioration of performance and lifetime due to radiation damage and the requirement of an energy storage system such as batteries. Solar panels and RTG can operate at the power output and duration necessary for this mission, but solar panels have a much lower specific cost and are generally safer, making solar panels the optimal choice.<sup>20</sup>

Because missions to Mars travel close to the Sun, panels with high specific powers are necessary to minimize the mass of the spacecraft. Many new technologies for solar panels are currently being researched. One new promising technology that is currently in use and being developed for space missions is Ultraflex Arrays, which have been shown to provide 295 W/m<sup>2</sup> of panel area and 115 W/kg of panel mass at 1 AU from the Sun. Another new technology are Stretched Lens Array SquareRigger (SLASR) solar panel arrays. The specific panel area and mass for both technologies at 1 AU from the Sun are shown in Table 14.<sup>22</sup> Also shown in Table 14 are the total mass and panel area that would be needed for the required 28 kW at 1.52 AU from the sun with 5% degradation of the panel effectiveness. Both technologies provide significant panel area and mass improvements compared to previous solar panel technologies. Both of these types of arrays have similar area specific power features, but using SLASR Arrays provides a huge mass advantage over the Ultraflex Arrays. With the SLASR technology the 28 kW needed can be achieved with solar arrays with a total mass of 184 kg and a total panel area of 215 m<sup>2</sup>.<sup>23</sup> The large solar panels will also be used for Mars aerocapture and must therefore withstand high levels of heat transfer. The selected solar panels are able to endure these high temperatures with only a decrease in efficiency during the course of the aerocapture. The performance will increase after the temperature decreases, when the aerocapture phase of the mission ends.

**Table 14. Comparison of Ultraflex and SLASR solar arrays.**

Cell Type	Mass Specific Power (W/kg)	Surface Area-Specific Power (W/m <sup>2</sup> )	Mass of Arrays for Mission (kg)	Area of Arrays for Mission (m <sup>2</sup> )
Ultraflex	115	294.7	574.43	224.16
SLASR	362	309	182.49	213.79

## 2. Batteries

Because the solar flux on the panels will not be constant, batteries are needed to store excess power for when the arrays are eclipsed from the sun. There are many battery types to consider. Common battery types for spacecraft include silver zinc, nickel cadmium, nickel hydrogen, and lithium ion batteries. Silver zinc batteries have a 30-90 day storage life, making them unsuitable for the MSRS. NiCad and NiH2 batteries are reliable and proven, given their long space heritage. Lithium ion batteries are more recently developed, so they are less proven but provide very significant mass and volume advantages. Lithium ion cells provide a 65% volume advantage and a 50% mass advantage over current nickel based batteries.<sup>20</sup> The large mass advantage makes lithium ion batteries the best choice for the mission. Using lithium ion technology, the battery mass for the mission is only 111.5 kg. Lithium ion cells also have other advantages over NiH2 cells, such as a higher charge efficiency and a larger range of operating temperatures.<sup>24</sup>

## 3. Distribution and Regulation

A sophisticated system is needed to manage and distribute the power between the solar arrays, batteries, and the spacecraft systems. Two types of regulation and distribution systems are common. Direct Energy Transfer (DET) systems dissipate unneeded power. Peak Power Trackers (PPT) extract the needed power from the solar arrays. DET systems are typically used for systems needing less than 100 W of power, so a PPT system is selected for this mission. A PPT system requires 4-7% of the power generated by the solar arrays to operate, increasing the required size of the solar arrays.<sup>20</sup>

# IV. Mars Descent Vehicle (MDV)

The MDV is the system that ensures that the MAV lands at the specified landing location on Mars without damage. The vehicle uses proven systems along with new systems that are ready to be tested

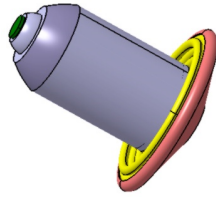


Figure 14. CAD model of MDV.

in a mission. The MDV will be released into the Martian atmosphere by the ITV, at which point it will deploy its different descent systems. In order, the systems chosen for this mission are a hypersonic inflatable deceleration device (HIAD), a supersonic parachute, and a scaled down version of the sky crane used during the Mars Science Laboratory (MSL) mission.

Table 15. List of technical requirements for the MDV.

Technical Requirements	Affected Systems
Safely deliver MAV to Martian surface	All Vehicle Systems
Accurately land MAV within 5 km of target	Navigation Systems
Capable of integration with ITV	Structural Design
Mass goal under 600 kg	All Vehicle Systems
Integration with MAV	Structural Design
TRL of 6 or above	All Vehicle Systems

### A. Systems Considered

Six options were considered for the Mars descent portion of the MSRS: parachutes, inflatable balloons, supersonic retropropulsion, airbags, and powered descent with a sky crane. Each option was rated against the parameters of accuracy, reliability, mass, feasibility, originality, simplicity, and cost. The MDV will enter the Martian atmosphere at 5.7 km/s, and the selected descent system must be capable of imparting sufficient  $\Delta V$  for the MAV to land safely.

Parachutes have been used in a large number missions and are therefore a very reliable option. Although they are not a comprehensive method of landing, because parachutes are not capable of imparting a large enough  $\Delta V$  for a safe landing, they can assist in the deceleration process. Parachutes involve very little mass, volume, and complexity, and are highly efficient.<sup>25</sup> With greater payload masses, larger parachutes are required to handle the larger loads and increase drag. However, the size of the parachute system is limited, because a parachute that is too large may rip in the turbulent flow, or fail to open. This can be solved by increasing the number of parachutes deployed, but this increases the complexity of the system, as well as the likelihood that the parachute lines will tangle and fail to deploy correctly.

Based on current findings from NASA, an inflatable balloon would open and “inflate” with martian air and expand due to the heat from the sun. A balloon requires less volume and mass than propulsion descent systems, and offers a controlled landing with low complexity.<sup>26</sup> However, it has only been tested with small payloads of 15 kg, and has never been tested for application similar to what is required for the MSRS.

Supersonic retropropulsion uses retro-rockets to increase drag.<sup>27</sup> It can be controlled for navigation and can handle a large payload mass. However, the system would be complicated and unsteady, and would result in a high mass due to the inefficiency of rockets. This concept raises a concern over the fluid flow and attitude control required to maintain a smooth descent, and requires additional heat shielding from plume coming back towards the vehicle. Additionally, these powerful rockets would create a large dust storm near the surface, therefore requiring that they maintain a reasonable distance from the ground, or that they be shut off before the final stage of descent. This can endanger the safety of the MAV.

An airbag system, similar to the Pathfinder and Mars Exploration Missions, was considered. Airbags would be used during the final portion of descent, inflating around the MAV payload just before impact with the surface. Airbags are simple, cost effective, and proven to be feasible. However, upon further analysis,

it was decided that landing the MAV in the correct orientation for launch using an airbag system would be difficult.<sup>28</sup> The integrity of the MAV is also important to the success of the mission, and the airbag system brings into question the safety of many sensitive components.

Most of the kinetic energy transfer in descent happens through friction during atmospheric entry. In the past, ablative heat shields have been used to slow descent vehicles to more manageable speeds. Ablative heat shields are known to be quite heavy, as they must have large surface areas to maximize drag and withstand large amounts of heat transfer.<sup>29</sup> NASA has been developing technology to replace ablative heat shields with inflatable materials that would decrease the overall mass of the entry vehicle. The system being considered for this mission would be used in the hypersonic region of descent, directly replacing the use of a heavier conventional heat shield. The Hypersonic Inflatable Aerodynamic Decelerator (HIAD) consists of multiple self inflated rings that deploy before atmospheric entry, covered in an ablative material blanket that would provide thermal protection from the heat experienced during atmospheric entry. This system would be utilized during initial entry into the Martian atmosphere, and would provide a tremendous amount of deceleration. The HIAD would provide a decrease in volume during storage, when a lower vehicle volume is desirable, but increase volume once deployed, when a larger surface area is desirable to increase drag. The HIAD system is a future technology being explored for its capability of landing larger and heavier payloads than ever before, with possible applications towards manned Mars descent. It is, however, less developed than many other descent methods, with a TRL of 6 and a lack of in-mission testing.

A tethered, automated powered descent system, known as the Sky Crane, was considered for this mission. This system uses monopropellant hydrazine engines to slow a landing vehicle at the last portion of descent, and then lowers the payload to the surface using three tethers and a data cable. This system was able to help the Curiosity rover touchdown with a velocity of 0.75 m/s, which is slower than any other previous Mars touchdown.<sup>29</sup> The Sky Crane uses throttleable liquid propulsion and an active guidance and control system to control velocity and position. Additionally, the ability to continue propulsion during the final stages of descent eliminates the dangers of free fall. Since the propulsion system is not positioned beneath the payload, very little dust is blown up into the air due to disturbances from the engines. The propulsion hardware and terrain sensors would be above the MAV payload as it is being lowered, so their operation would be able to continue uninterrupted, which improves landing accuracy and safety, as well as velocity control. However, it is a complicated system with multiple autonomous components, which reduces the system reliability and increases complexity. The Sky Crane is also a massive, complicated, and expensive system that would require a large amount of propellant and storage space in the MDV.

## B. Design Decision

After detailed consideration, the HIAD, parachute, and Sky Crane were chosen as the systems that would carry the MAV to the martian surface. Using the decision matrix below, each system was rated based on criteria that was deemed important for mission success and optimization. Each category was assigned a weight from 1 to 5, which represented the importance of that category for mission success. The scores for each system were multiplied by their weights and totaled in order to outline the feasibility of each system. For the MSRS, the three systems with the highest totals were chosen for integrated use as the descent system.

**Table 16. Descent method decision matrix.**

Criteria	Propulsion	Airbags	Balloons	Sky Crane	Parachute	HIAD	Weight
Accuracy	5	1	4	5	3	3	4.8
Reliability	5	2	2	4	4	3	4.4
Mass	1	5	5	1	1	5	5
Feasibility	3	2	2	5	5	4	5.0
Originality	2	3	5	3	2	4	2.7
Simplicity	3	4	3	3	4	3	2.1
Cost	1	4	3	1	5	2	1.0
Total	76.9	61.5	78.0	85.2	93.1	84.0	

### C. Structures

The MDV can be separated into a number of subsystems: the parachute, backshell, Sky Crane and MAV, MAV payload bay, and the HIAD system and adapter.

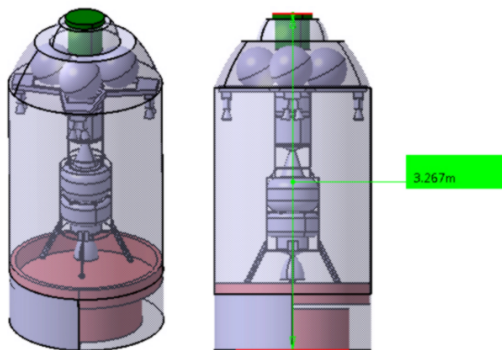


Figure 15. CAD model of MDV.

Table 17. Total mass breakdown for MDV.

Component	Mass (kg)
Structures	105
Heat Shield	20
Parachutes	50
Sky Crane	214
Propellant	135
Total Mass	524

#### 1. Parachute

The parachute is intended for the supersonic portion of descent. It is positioned on top of the backshell when stowed, and designed to model the MLS parachute. Given that the MSRS parachute will have a nominal diameter of 115 m, Table 18 can be used to determine the deployed parachute dimensions. The parachute will use a mortar deployment system, which is used to eject the parachute at the correct velocity range so there are no problems with line entanglement and parachute failure. The parachute system will be 50 kg.<sup>30</sup>

The MDV will use a disk gap band parachute with a nominal diameter of 15 m, based off of the parachute used during the Opportunity landing.<sup>29</sup> The parachute canopy will have a high segment, or gore, count of 80, based on MSL architecture, in order to spread loads across more fabric, since the parachute will have to withstand loading and reloading during opening and descent. The parachute canopy will be made of nylon fabric and a Kevlar base in order to maximize strength.<sup>30</sup>

#### 2. Backshell System

The backshell is an integral part of the MDV that houses the parachute and Sky Crane, as well as providing a point of attachment between the MDV and ITV during interplanetary travel. After cruise phase, the MDV will detach from the ITV via pyrotechnics, at which point its attitude will need to be oriented for the desired entry path. The MDV will use four sets of hydrazine thrusters, oriented on the backshell in order to alter its attitude when necessary. About 15 kg of propellant will be used for attitude control.<sup>31</sup> The backshell has a minimum diameter of 0.5 m at the top, is the attachment point of the parachute system. The maximum diameter of the backshell is 1.5 m. The size of the backshell is dependant upon the maximum diameter of the Sky Crane system, in order for it to be safely contained within the vehicle. The backshell has a total height of 0.668 m to account for the parachute system mounted on top.

**Table 18. List of dimensions based off of MSL Parachute system.<sup>30</sup>**

Nominal Diameter ( $D_0$ )	19.7 m
Disk Diameter	$0.72D_0$
Reference Area	$0.25\pi D_0^2$
Geometric Porosity (Area)	12.5%
Vent Diameter	$0.07D_0$
Band Height	$0.121D_0$
Gap Height	$0.042D_0$
x/d	10
Suspension Line Length	$1.7D_0$

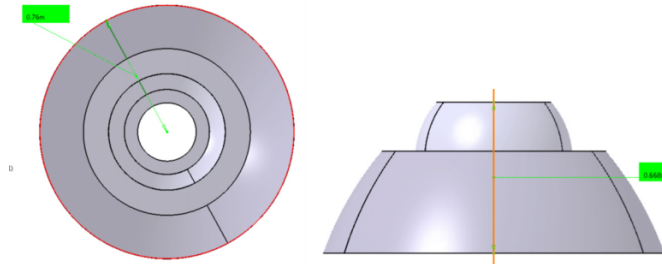


**Figure 16. Top and side view of backshell.**

### 3. Sky Crane Design

Similar to the MSL Sky Crane, the MSRS Sky Crane will attach to the MAV payload with three Kevlar straps, which will attach above the center of mass, in order to prevent tipping. The Sky Crane is equipped with eight monopropellant hydrazine Mars Lander Engines that are angled away from the payload, promoting stability and decreasing the effect of the exhaust plume on the payload. Only four of the eight engines are active during the Sky Crane landing, and each engine is capable of 400 to 3000 N of thrust. A scaled down version of the MSL Sky Crane system will be used for terminal descent for this mission. The MSL Sky Crane had a mass around 642 kg, plus 390 kg of propellant.<sup>32</sup> Since the mass of the MSL was 899 kg, and the MAV is 288 kg, it was estimated that the MSRS Sky Crane would need a third of the propellant and structures. This leaves the MSRS Sky Crane to have 214 kg of structures and 120 kg of propellant.

### 4. Payload Bay

Unlike Curiosity, the MAV cannot fit within the parameters of a backshell. In order to protect the MAV from radiation during interplanetary transport and the atmospheric effects experienced during entry and descent, as well as to connect a heat shield to the backshell, a cylindrical structure is implemented between the heat shield and backshell. After parachute deployment and before the Sky Crane is dropped from the backshell, the payload bay is separated from the backshell using pyrotechnics.

The size of the payload bay is limited by the height of the MAV and the diameter of the Sky Crane. The payload bay is designed to house a MAV that is 2.1 m tall and a Sky Crane that is 1.5 m wide. The resulting structure is 2.25 m tall and estimated at 105 kg. The MDV payload bay must survive Earth launch and Mars entry. In order to maximize the strength and minimize the weight, a titanium alloy was chosen as the payload bay material.

### 5. Inflatable Heat Shield

The HIAD was chosen as a replacement for a rigid heat shield. The inflatable rings of the HIAD are made of sturdy Kevlar fibers bonded to the surface of a film. This film would envelope a barrier that would contain the gas used to inflate each ring.<sup>33</sup> Both the inflatable rings and the TPS blanket must be flexible to withstand the forces during the hypersonic portion of the descent. Research indicates that a TPS made of

two layers of SiC fabric, two layers of Pyrogel 3350, and two layers of Kapton is able to survive  $100 \text{ W/cm}^2$ , which is greater than the peak flux of  $44 \text{ W/m}^2$  experienced during the Opportunity entry.<sup>34</sup>

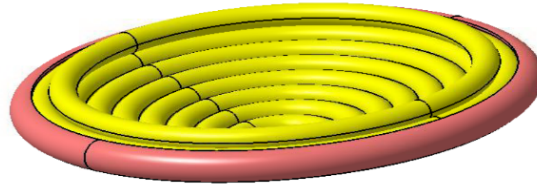


Figure 17. Concept Design of HIAD.

During transit, the HIAD system will be stowed under two titanium half cylinders that will protect the system. These casings will be jettisoned right before the HIAD is inflated. The HIAD will be positioned at the bottom of the MDV, connected to the MAV payload bay. The entire HIAD assembly is 20 kg, based on a 9 m diameter inflatable heat shield outlined in Fig. 18.<sup>33</sup> The MSRS HIAD will have a diameter of 2.65 m with an angle of  $70^\circ$ , as per the dimensions used for the heat shield of the Opportunity descent, due to the similarities in payload masses.<sup>29</sup> Included in this mass is the gas used to inflate the rings, gas generator, and a system used to regulate ring inflation.<sup>33</sup>

**Table 2 Nominal parameters and mass breakdown for architecture 2**

Variable	Value	Components	Mass, mT	%	Areal Density, kg/km <sup>2</sup>
Diameter, m	23.0	Adapter	2.2	21.2	5.3
Heatshield diameter, m	9.0	Heatshield	1.1	10.2	2.6
Aerocapture Heat Load, MJ/m <sup>2</sup>	87.3	Inflatable	1.8	16.8	4.2
Entry Heat Load, MJ/m <sup>2</sup>	26.1	Avionics	0.1	0.9	0.2
Max Dynamic Pressure, Pa	4240.1	Separation	1.3	12.4	3.1
Payload Mass, mT	40.0	TPS	4.0	38.5	9.7
Arrival Mass, mT	83.6	Total	10.5	100.0	25.1
HIAD Mass, mT	10.5				

Figure 18. Mass estimates for 9 diameter HIAD system.

## D. Navigation

One of the biggest challenges of this mission will be configuring the guidance, navigation and controls (GN&C) of the MDV during entry, descent, and landing (EDL). A landing accuracy of within a 5 km radius represents the next generation of MDV and will require advanced GN&C to function. Hazard avoidance will also require robust GN&C to ensure the safety of the MAV during landing.<sup>35</sup> For the purpose of this mission, several Monte Carlo simulations were executed for a number of different scenarios to determine the initial conditions and controls required during the approach phase of the entry trajectory.

### 1. Background

The descent is made difficult by the Martian atmosphere, which is thick enough to cause substantial heating but not thick enough to provide low terminal descent velocity.<sup>36</sup> Furthermore, the complex surface of Mars presents a number of hazards to the final stages of descent. The entry trajectory of the MDV can be broken into four categories: approach phase, entry phase, chute phase, and powered descent phase.<sup>29</sup> The approach phase encompasses the interplanetary transfer up until the MDV is deployed and reaches an altitude of about 125 km. The hypersonic entry phase encompasses the entry up until parachute deployment, at which point the MDV will shift into the chute phase. Finally, the powered descent phase starts when the Sky Crane ignites its engines, and lasts until the MAV has safely reached the ground. For the purpose of this study the hypersonic entry phase was analyzed the most.

### 2. Numerical Model

First, a numerical model was developed for determining the state of the MDV at various times during the descent.<sup>37</sup> This was done using equations of motion considered in a 2-D reference frame. The vertical velocity



$$\dot{h} = V \sin(\gamma)$$

and the horizontal velocity

$$\dot{x} = V \cos(\gamma)$$

are both defined with respect to the local frame. The absolute acceleration

$$\dot{V} = \frac{-\rho V^2}{2B} - g \sin(\gamma)$$

where B is the ballistic coefficient, was derived from a sum of forces,

$$\dot{\gamma} = \frac{-\rho V \frac{L}{D}}{2B} + \frac{g \cos(\gamma)}{V} - V * \cos(\gamma)$$

is derived from kinematic relationships. Once a model was developed for the MDV motion, a model had to be developed for Martian atmosphere. A simple scale height model was used for the atmosphere,

$$\rho = \rho_0 e^{\left(\frac{-h}{H}\right)}$$

where the scale height, H, was determined using the following equation:

$$H = \frac{kT}{mg}$$

where k is Boltzmann's constant, T is the temperature, m is the average mass of atoms in kilograms, and g is the gravitational acceleration.

For the purpose of this study, wind force was neglected. In addition, the MDV descent was simplified to a process that did not include the hypersonic parachute system. Out of plane motions were neglected; however, a majority of the MDV motion does occur in a 2-D plane, and would likely not result in the MDV missing the target. Furthermore, the use of a scale height atmospheric model assumes that the atmosphere of Mars is 100% CO<sub>2</sub>, and that the gas behaves ideally.

### 3. Simulations

Once models of the trajectory and atmosphere were devised, a simulation was developed using specifications from the MDV and the Martian environment. A summary of the initial simulation inputs is in Table 19.

**Table 19. Summary of model initial inputs.**

V (km/s)	5.5
Alt (km)	125
L/D	0.23
B (kg/m <sup>2</sup> )	139
K	1.38e-23
T(K)	210
M (kg)	7.3e-26

Multiple Monte Carlo simulations were run to determine the acceptable initial flight path angle and command logic that the MDV should use to hit the targets. Initial flight path angles were ruled out based on whether or not they could reach the target ellipse, and whether this could be done without violating a lift to drag ratio (L/D) range of 0.18 to 0.3.<sup>37</sup> An initial, un-guided test of the model was run with varying initial flight path angles and a constant L/D to better match the decided upon target with acceptable ranges of initial flight path angles.

To implement a guided trajectory, a function was developed to analyze the course of the MDV and alter the L/D of the MDV if the current trajectory was off course. Several scenarios were devised with targets at different downrange distances to test the model. A sample result for a downrange target of 1800 km is displayed in Fig. 20.

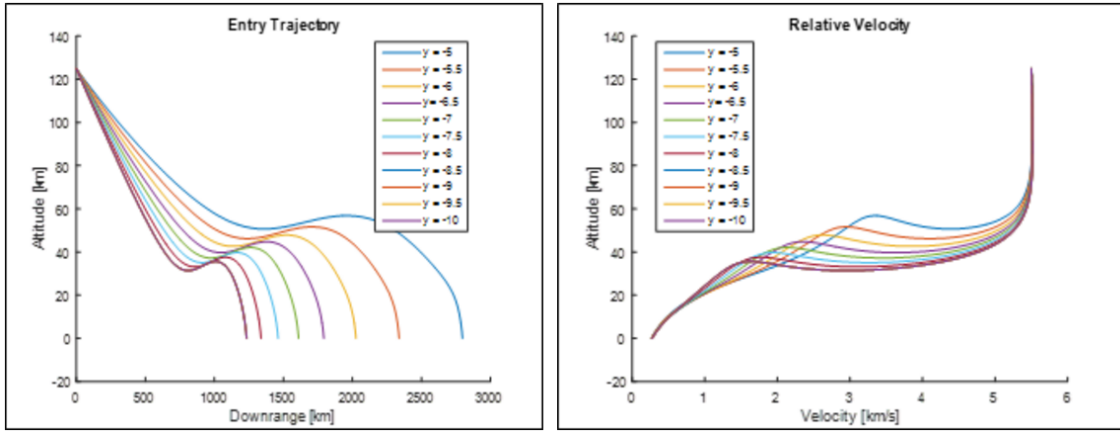


Figure 19. Results of unguided test.

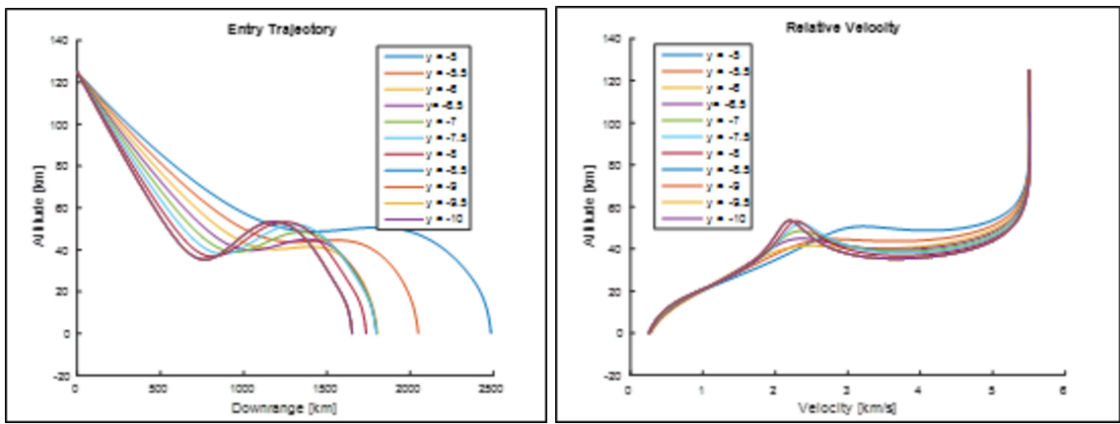


Figure 20. Guided flight paths for target of 1800 km downrange.

While the MDV was capable of navigating to the target for a majority of initial flight path angles, the MDV was not capable of guiding itself to the target when on a flight path lower than  $6^\circ$ . Theoretically, the GN&C could guide those cases to the target given enough opportunities to compute course corrections; however, the resulting L/D was pushed to unrealistically low values. Therefore, for guidance to an 1800 km downrange target, any flight path below  $6^\circ$  was deemed infeasible. Fig. 21 illustrates the MDV miss distance for acceptable flight path angles.

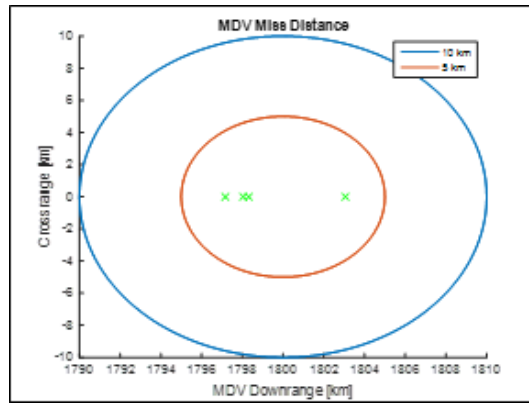


Figure 21. Illustration of the MDV miss distances.

A summary of the results of the various scenarios is provided in Table 20. The acceptable flight path angles for each scenario are provided with the most accurate paths falling in the middle of the given range.

Scenario 1 and 4 were conducted to test the extremes of the GN&C. While scenario 1 was successful, scenario 4 was unsuccessful because a number of the trajectories were flying at such a low flight path angle that they skipped off of the upper atmosphere as shown in Fig. 22. The additional trajectories failed to stay within the acceptable limits for L/D.

**Table 20. Summary of scenario results.**

Scenario	Downrange Distance to Target (km)	Acceptable Flight Path Angles (°)
1	1000	-12 to -8.5
2	1500	-8.5 to -4.5
3	1800	-7.5 to -6
4	2100	Unachievable

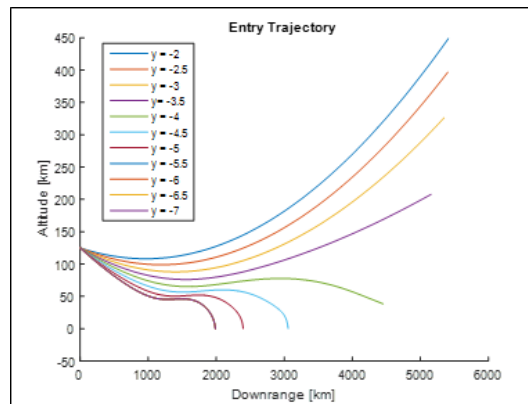


**Figure 22. Entry trajectory for low flight angles.**

Another key issue during EDL is hazard avoidance, which will have a significant impact on the success of the mission. Hazards such as large rocks, uneven surfaces, and slopes pose a significant threat to the MAV. For a legged system, such as MAV design for Project Argonaut, surface variability poses the most hazard with a 2-15% probability of causing a failure.<sup>29</sup> In addition, with only 5 cm of clearance between the nozzle and the surface, landing on a smooth surface within the target ellipse will be critical to mission success. Usually hazard avoidance is performed during the powered descent phase;<sup>38</sup> however, the powered descent phase can only move 100 m to avoid hazards.<sup>35</sup> Due to the significant threat ground hazards pose to mission success, basic studies were conducted to determine if the GN&C could provide some hazard avoidance during the entry phase. This was done by placing hazards in the path of the MDV inside the target ellipse. For example, a 1 km radius hazard was inserted into the target ellipse. A sample result of the code with hazard avoidance functions implemented is provided in Fig. 23.

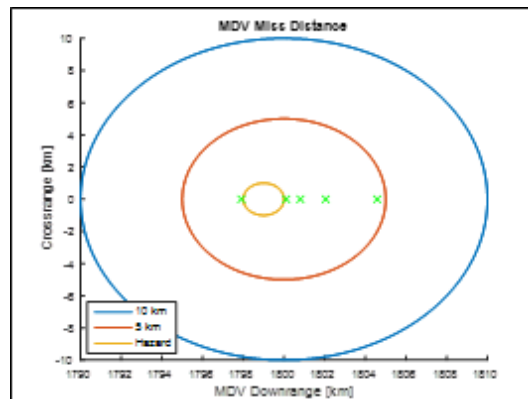


**Figure 23. MDV target ellipse with hazard.**

#### 4. Results

These simulations make it apparent that an extensive knowledge of the target landing location is required before the MDV begins approach. The downrange distance of the target and the kind of hazards present within the target ellipse would need to be known ahead of time to prevent mission failure. This would demand that ample time is spent before EDL analyzing the desired targets and mapping out hazards. Furthermore, an in-depth analysis of the Martian environment, including a wind and atmospheric model, would be required.

A surprising result from these studies was the effect minute changes in L/D had on the final downrange distance of the MDV. This suggests that a finer control over the MDV thrusting during EDL could provide a more accurate landing, and may actually be necessary to meet future EDL accuracy requirements. In addition, it illustrates a key trade-off that has to be made during the algorithm design process.

The algorithm has to be designed to either allow for incredibly accurate L/D alterations, or an increased number of opportunities to analyze whether or not the MDV is on course. Making minute changes to the L/D may prove unfeasible from a design perspective, meaning the number of times the MDV checks course would need to be increased. However, this is computationally stressful, and may also prove difficult from a design perspective. In addition, the MDV would have less than 5-8 minutes to complete these calculations, which means that the on-board guidance system would have to be very advanced. Thus, a balance between the two trade-offs would need to be established.

While this model provides useful information about the MDV descent and illustrates that landing within a 5 km radius of a target is feasible given proper GN&C software, there are still a number of uncertainties that need to be addressed in more advanced models and simulations. The largest of these uncertainties is the atmospheric model of Mars. There have been many efforts to reconstruct the atmosphere from EDL data acquired during the MSL descent.<sup>39</sup> Furthermore, there are a number of performance penalties that are associated with guided entry. Carrying extra propellant to perform the maneuvers during entry either reduces the scientific payload or constrains the landing sites the MDV is capable of reaching.<sup>40</sup>

#### E. Entry, Descent, and Landing Description

Once the ITV is captured into Mars orbit, the MDV will be deployed using pyrotechnic separation. The attitude of the MDV is then adjusted for the desired flight path. The HIAD casing is jettisoned, and the heat shield inflates before the MDV begins descent into the Martian atmosphere. The HIAD will experience temperatures as high as 2,100°C, and will provide a large majority of the deceleration required during descent by decreasing the MDV velocity to less than 1 km/s. Attitude corrections will provide navigation control and orient the vehicle to produce lift during the fall. Once the MDV is approximately 11 km from the surface, the parachute is deployed to increase the drag of the craft. At approximately 8 km from the surface, the HIAD detaches from the payload bay and drops away. With the payload bay exposed in the direction of the surface, the radar, camera, and navigation systems will be able to calculate the speed and altitude of the MDV before it begins powered descent. The Sky Crane is then detached from the payload bay and parachute, and its thrusters are ignited. The Sky Crane retrorockets divert out of the descent path of the separated backshell and perform a controlled descent towards the surface. At an altitude of just under 300 m, the Sky Crane slows descent and shuts off half of its engines, before lowering the MAV the last 10 m with three nylon tethers and a data cable. When the MAV touches down and the descent stage registers the reduced strain in the cables, the suspension lines are cut, and the Sky Crane flies to a safe location at least 150 m away from the MAV for impact.<sup>41</sup>

### V. Mars Ascent Vehicle (MAV)

The MAV is one of the most technologically challenging components of the MSRS, particularly considering no part of this system has been tested before in a mission. The MAV will be deposited on the Martian surface by the MDV, and must then survive in the harsh Martian environment for at least 50 Earth days as the science rover transports the sample cache to the landing location. Once the MAV has collected the sample, it will launch into a circular orbit of 500 km to transfer the cache to the ITV.

This section discusses in detail the selection of a propulsion system, communications system, thermal control system, power system, and structural design for the MAV. The overall design of the vehicle is constrained by requirements in size, weight, accuracy, reliability, and the environment in which it will be placed. Additionally, it is important that planetary protection is considered in designing the MAV, in

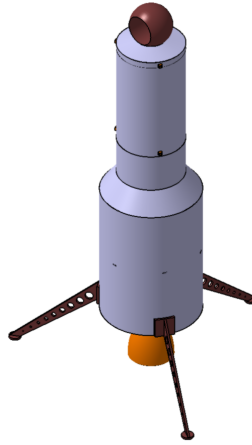


**Figure 24. Isometric view of MAV.**

order to minimize the impact that this mission will have on the Martian surface in terms of damage and contamination. These requirements and the resulting dependencies are outlined in Table 21.

**Table 21. List of technical requirements for the MAV.**

Technical Requirements	Affected Systems
Minimize mass below 300 kg	All Vehicle Systems
Survive on Mars surface for at least 50 Earth days	Thermal Control System, Radiation Protection System, Power System
Fit within dimensions of MDV	Propellant Tank Sizing, Engine Sizing and Selection, Structural Design
Launch into 500 km orbit	Engine Thrust Selection, Propulsion System, Trajectory Guidance System
Receive sample cache less than 2 m above surface	Structural Design
Hold sample container cylinder	Structural Design, Propulsion System
TRL of 6 or above	All Vehicle Systems
Minimize environmental impact on Mars	Propulsion System

## A. Propulsion

Multiple different propulsion systems and propellants were considered for use on the MAV. The options were evaluated primarily on their mass requirement, with the goal of keeping the overall MAV mass below 300 kg, as well as on their reliability. Along with a theoretical comparison of each system considered, a numerical comparison was made based on the overall vehicle mass required for each system. In choosing the propulsion system for the MAV, a trade study was conducted between different propellants, including liquid, solid, hybrid, and gel, as well as between different numbers of stages.

### 1. Liquid Propellants

Liquid engines have a high  $I_{sp}$  due to the use of liquid oxidizer, as well as throttling, shutdown, and restart capabilities. In order to perform a precise orbit injection, the variable thrust capabilities of liquid propulsion may be necessary. However, liquid propellants are difficult to store, requiring specific pressures and temperatures. This would necessitate a TPS, as well as a system of valves, seals, pipes, and turbopumps.<sup>42</sup> Some liquid oxidizers are even unstable and toxic, which complicates the construction of the MAV, and leaves the potential for harmful contamination of the sample and the surface of Mars. Scaled versions of the SpaceX Kestrel, RL-10, TR-201, Lunar Descent, ATE, and AJ10-190 engines were compared using different numbers

of stages and different combinations of engines.<sup>43</sup> These engines were scaled based on the required thrust using the square-cube law presented in Comments on Rocket Scaling.<sup>44</sup> Of these options, the SpaceX Kestrel resulted in the lowest final MAV mass for both a one stage and two stage system.

## 2. *Solid Propellants*

Solid propellants have a much higher density than liquid or gas propellants, which would reduce the volume of the MAV. Some drawbacks of solid propellants are their lower  $I_{sp}$ , and their inability to be throttled, shutdown, or restarted. Solid propellants are also very sensitive to the conditions in which they are kept, because they are intolerant to cracks and voids that may occur as a result of their storage temperature.<sup>42</sup> This means that sufficient thermal protection from the Martian environment would be necessary to ensure the functionality of the propulsion system. Of the solid engines considered, the Altair 3, Star 17A, and Star 13A engines proved most promising.<sup>43</sup> A combination of the Star 17A and the Star 13A engines in a two stage system resulted in the lowest MAV mass for a solid propulsion system.

## 3. *Gel Propellants*

The option of gelled propellants was considered for its benefits related to storage, safety, and performance. Gelling liquid propellants results in a lower vapor pressure, which reduces the risk of accidental ignition and provides many of the storage benefits of solid propellants. Additionally, gel propellants behave similarly to liquid propellants in flight, with a high  $I_{sp}$  and the capability of being throttled and controlled. The propellant and exhaust gas are also safe and non-toxic, which reduces the possibility of contamination.<sup>45</sup> Unfortunately, gelled propellants are still very early in the research and development phase, and it is uncertain whether gelled propellant technology would be ready by 2020.<sup>46</sup>

## 4. *Combination Solid and Liquid Propellants*

A MAV using solid propellant for the first stage and liquid propellant for the second stage was also considered. This system would provide a middle ground for some of the advantages and disadvantages of solid and liquid propellants. One major benefit of this system would be combining some of the mass and cost benefits of solid propellants with the capability of throttling and controlling trajectory during the upper stage, which would allow corrections to be made for the inaccuracy of the solid stage trajectory and result in a more precise orbit insertion. A MAV case was calculated using the first stage engine of the selected solid propulsion design, the Star 17A, along with the selected liquid propellant engine, a scaled SpaceX Kestrel.<sup>43</sup>

## 5. *Hybrid Propellants*

Hybrid rockets use a solid fuel and liquid or gas oxidizer. Because the oxidizer is fluid, hybrid rockets can be throttled, shutdown, and restarted, and they also have a high  $I_{sp}$ .<sup>47</sup> Hybrid systems only involve a single fluid propellant, which allows for simple storage systems and throttling operations.<sup>48</sup> Deterioration in storage is also not an issue with hybrid propellants, which is necessary for the MAV to remain operational after 50 days on Mars.<sup>49</sup> The fuel grains used in hybrids are robust and insensitive to cracks, debonding, imperfections, and environmental temperatures. This gives hybrids a higher fault tolerance than solid propellants, and eliminates the requirement of quality control operations such as thermal protection.<sup>50</sup> However, one major issue with hybrid propellants is the low fuel regression rate, which causes lower gas generation and thrust. A proposed solution to this problem involves the use of complex multi-port designs, which provide increased thrust, but leave residual slivers of propellant and add complexity. Hybrids have also undergone less development than solid or liquid engines, and have only been used in one flight-production application.<sup>48</sup> Although research and testing have been conducted on hybrid propulsion, some advancement is still needed before the technology is completely mission-ready.<sup>46, 49, 51</sup>

Despite these problems, most of the disadvantages associated with hybrid propulsion can be overcome with design solutions. Recently, several new methods have been developed that can improve the regression rate and TRL of hybrids through oxidizer flow modifications, the addition of energetic materials to the fuel grain, and the use of alternative fuels such as paraffin wax.<sup>47</sup> From research, a hybrid rocket propulsion system using Nitrox oxidizer and paraffin-based fuel with aluminum loading proved most optimal.<sup>46, 50, 52</sup> Paraffin fuels have a high regression rate, and can produce desirable thrust levels using a simple single circular port grain design. Paraffin fuels are also hydrophobic, which makes them an ideal binder for metals such as

aluminum powder. This aluminum addition gives the hybrid a higher  $I_{sp}$  and density, and lowers the O/F, reducing the oxidizer tank size and resulting in less mass.<sup>46</sup> The oxidizer, Nytrox, is a mixture of nitrous oxide and oxygen that combines the high vapor pressure of dissolved oxygen with the high density of cooled nitrous oxide. At a given temperature, the Nytrox density remains mostly constant with pressure, which provides flexibility in selecting the system pressure. However, over the course of the burn, the Nytrox requires some pressurization in order to maintain the optimal oxidizer flow rate. Using oxygen as the pressurant enables nearly complete utilization of tank ullage. As the oxidizer tank empties and the mixture transitions from liquid nitrous oxide to mostly gaseous oxygen, the resulting decrease in the oxidizer mass flow rate also decreases the operational O/F. Coincidentally, the optimal O/F ratio for a burn with paraffin and nitrous oxide is higher than that of paraffin and oxygen, and therefore the downward shift in operational O/F allows the propellant to burn until nearly all of the pressurant is depleted. A final advantage of these propellants is their compatibility with the temperatures on Mars. Paraffin has a low glass transition temperature and weak transition.<sup>46</sup> Therefore the fuel should be able to recover even from temperatures below glass transition. Additionally, Nytrox can be chosen to match the expected temperatures on Mars, and its performance increases with decreasing temperature.<sup>52</sup> In this way, hybrid propellants allow the design to take advantage of the cold Martian environment rather than fighting it with thermal controls.

## 6. Number of Stages

A trade study was also completed on the optimal number of stages for the MAV. Because of the small payload and low  $\Delta V$  requirement of the mission, it was determined that having more than two stages would add unnecessary complexity due to the required staging interfaces and separation mechanisms. For every propellant option, a two stage system provided substantial overall mass savings over a one stage system, making the necessary interstage complexity worthwhile. For reference, a single stage liquid propulsion system using a scaled SpaceX Kestrel engine was added to the comparison in Table 22.

## 7. Design Decision

The payload of the vehicle, in order to create a fair comparison between different propulsion systems, is taken to be 36 kg. This consists of the 3 kg sample cache, as well as the stage interface and separation mechanisms, avionics, telecommunications, cabling, basic thermal control, structure, RCS, and a 14% contingency. This estimation is assumed sufficient based on discussions with JPL personnel cited in a systems study conducted by Stanford University and Space Propulsion Group, Inc. Each system mass was calculated to obtain a conservative  $\Delta V$  of 4.375 km/s, which is more than sufficient to reach a 500 km circular orbit, and should leave room to account for the uncertainty of drag losses, changes in landing sites, and any required thrust vectoring.<sup>50</sup> The landed mass was calculated by adding the mass of the appropriate landing base for each system. For every propulsion option except the hybrid, thermal protection is necessary to ensure the functionality of the propellant. For these systems, the base is assumed to include an erector integrated with a TPS termed the “igloo”, taken to be 35 kg from NASA designs.<sup>31</sup> For the hybrid propulsion system, a base of 15 kg was added to the overall mass, consisting of a leg system extending from the bottom of the MAV.

Once the mass of the lander and thermal control are added to each MAV, the two stage hybrid design results in the lowest overall mass. Although the solid and liquid options have a more desirable TRL, these designs are less optimal. The hybrid system is capable of precision orbit insertion, trajectory optimization, enhancing mission flexibility, and operating within a very broad range of conditions. Hybrid propulsion technology will require a substantial development program in order to be mission-ready by 2020, but it meets all criteria for the MSRS and provides many advantages over other propulsion systems in safety, cost, mass, and complexity.

The chosen propulsion system for the final design of the MAV is a two stage, pressure-fed hybrid rocket using Nytrox60 oxidizer and paraffin-based fuel with 40% aluminum loading by mass. This MAV design is outlined in a system studies conducted by Stanford University and Space Propulsion Group, Inc. for use within MSR mission architecture.<sup>46,50,52</sup> The optimal system has a  $\Delta V$  distribution of 1.675 km/s for the first stage and 2.700 km/s for the second stage, with a stage one to stage two mass ratio of 1.53. The Nytrox60, or Nytrox at  $-60^{\circ}\text{C}$ , is stored in separate tanks as  $\text{N}_2\text{O}$  and  $\text{O}_2$  until a few sols prior to launch, at which point the oxygen gas is transferred to the main oxidizer tanks to make equilibrium Nytrox. The Nytrox mixture is 15% oxygen by mass in the liquid phase and 65% oxygen by mass in the gas phase.<sup>46</sup> The design assumes a conservative structural coefficient with a mass contingency of 40% on all structural

**Table 22. Comparison of selected MAV propulsion systems.**<sup>43, 50</sup>

Propulsion System	Single-Stage Liquid	Two-Stage Liquid	Two-Stage Solid	Solid and Liquid	Two-Stage Hybrid
Stage 1 Thrust (kN)	7.75	7.75	16.01	16.01	8.21
Stage 1 $I_{sp}$ (s)	371	317	287	287	301
Stage 1 Mass (kg)	257.8	150.0	215.6	150.6	145.9
Stage 2 Thrust (kN)	—	7.75	5.87	7.75	3.83
Stage 2 $I_{sp}$ (s)	—	317	287	317	303
Stage 2 Mass (kg)	—	78.3	50.2	98.2	91.4
Payload Mass (kg)	36	36	36	36	36
MAV Mass (kg)	293.8	264.3	301.8	284.8	273.3
Base System Mass (kg)	35	35	35	35	15
Landed Mass (kg)	328.8	299.3	336.8	394.8	288.3

components.<sup>50</sup> The chosen hybrid design also meets standards for planetary protection since it poses no threat to the Martian environment.<sup>46</sup>

The technology developed for a hybrid MAV provides significant mission flexibility that allows it to accommodate future Mars missions, as well as be applied to ascent vehicles on other planetary missions and in-space propulsion. Small hybrid motors such as those modeled for the MAV design are expected to finish development within a two to three year period with a low level of investment.<sup>49</sup> Hybrid propulsion could therefore easily be developed to the point of mission readiness in time for the proposed MSRS. Hybrid rocket propulsion is a tipping point technology that could provide game changing developments for future space mission propulsion with very little effort. This could prove to be a stepping stone to future human planetary ascent vehicle development.

### 8. Attitude Control System

Attitude control will be necessary to control the direction of thrust of the MAV as it ascends, as well as to provide a more accurate orbit insertion. In order to maintain the benefits in mass and system complexity provided by the main hybrid propulsion system, liquid RCS engines were not chosen for the design. Instead, the first stage will use thrust vector control through gimbaling for steering. A hybrid rocket RCS system was chosen for the second stage to preserve low system complexity. This system uses the same propellants and grain structure to a smaller scale, containing six hybrid micro-thrusters with force capabilities between 5 and 50 N. Each thruster would be able to burn for over a minute, and their thrust would be controlled through the oxidizer flow. The thrusters would be organized into three pairs around the MAV, with one pair each for yaw, pitch, and roll rotation.<sup>53</sup>

## B. Structures

Using the estimations from Table 22, parameters for the volumes of fuel, oxidizer, and pressurant were calculated in Table 23 and then used to create a CAD model of the MAV. In addition, the housing structures, landing legs, nozzles, and aeroshells were modeled in Fig. 25.

**Table 23. Volumes of propellants in MAV model.**

Propellant	N <sub>2</sub> O (Oxidizer)	O <sub>2</sub> (Pressurant)	Paraffin (Fuel)
Stage 1 Volume (m <sup>3</sup> )	0.0548	0.0245	0.0214
Stage 2 Volume (m <sup>3</sup> )	0.0193	0.0112	0.00964

The sample cache will be placed inside a protective sphere attached to the top of the MAV, such that it survives staging operations as it is launched and does not affect the MAV center of mass. A preliminary design proposed for the sample cache to be attached to one of three fins located at the bottom of the MAV



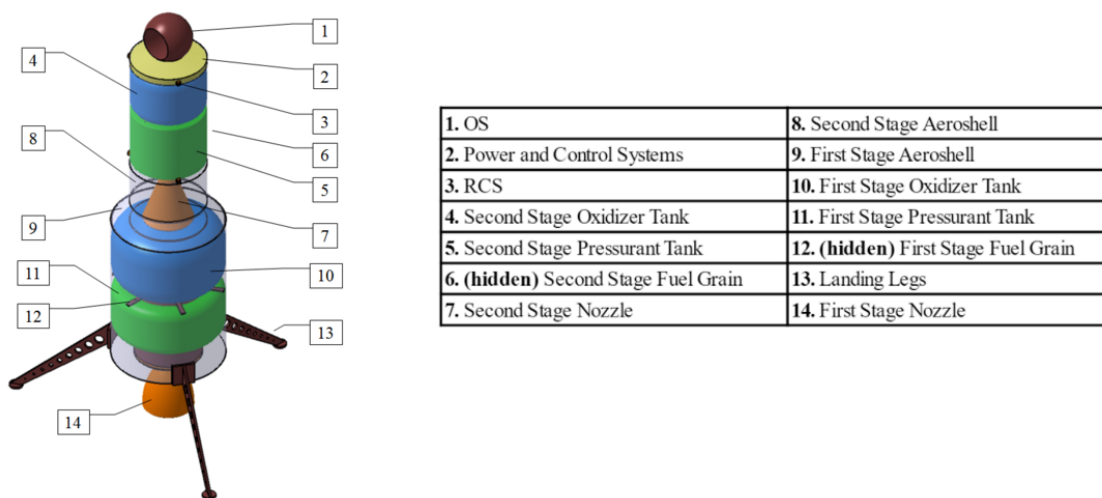


Figure 25. Isometric view of MAV interior with labels.

structure in order to keep the height of the MAV form being constrained by the range of the rover. This design would limit the MAV to one stage, and require more complex systems for the sample to be transferred to the ITV. For these reasons, a two stage rocket with a maximum height of 2 m was adopted. An additional constraint of a 1.5 m diameter is also imposed due to the specifications of the MDV. For the rocket to meet the height limit, components were designed to be short and wide. Oxidizer containers are near spherical to limit height and also minimize the surface area. Pressurant tanks were designed in the shape of tori and wrapped around the solid fuel grain to condense the design as depicted in Fig. 26. However, hybrid engines are built to have long fuel grains to more efficiently burn. The final design is 1.99 m in height, allowing the rover to place the container within the top of the MAV. The legs extend out to the 1.5 m diameter limit in order to provide maximum stability. Three low-mass legs are used to create a stable triangle. They extend only 5 cm beyond the bottom of the first stage nozzle to minimize excess material. The landing navigation system will identify the smoothest and least inclined spot to touch down, such that the legs do not require sensors and adaptive motors. The aeroshell and fuel containers are constructed from aluminum to minimize the structural mass. Pressurized components, such as the oxidizer and pressurant tanks, have wall thicknesses of 5 mm, and the aeroshell has a thickness of 2 mm due to the thin Martian atmosphere.

Depending on the selected landing site for the MSRS, the MAV might be required to launch into an orbit inclination that is different than the launch latitude. To account for this, an analysis was performed to determine the sensitivity of the propellant mass usage to the angle at which the MAV is launched. The results indicated that the required propellant mass is largely insensitive to variation in the initial launch angle, with a less than 1 kg difference in the vehicle gross mass at lift-off between the most and least optimal angles.<sup>55</sup> For this reason, it was determined that an erector and launch tube system is not necessary to set up the launch of the MAV. After launching at 90°, any extra propellant required for inclination corrections can be easily accounted for in the  $\Delta V$  contingency already applied to the propulsion design.

### C. Thermal

One of the biggest challenges for the MAV design will be surviving the cold and highly variable environment on Mars. Holden Crater was the candidate MSL landing site with the most temperature variation, ranging from -111°C to 24°C. The MAV was therefore designed to be capable of surviving within this worst-case scenario environment. The average surface temperature over a Martian year is about -60°C.<sup>50</sup> The functionality of the MAV depends on maintaining thermal conditions within the operational limits of the batteries, electronics, and propellant while the MAV is located on the Martian surface. The propulsion system is designed to require minimal thermal control, which greatly reduces the mass and complexity of the TPS. With the average annual temperature on Mars at -60°C, thermal protection will certainly be necessary to ensure the safety of all mission-critical components.

The MAV will contain some of the typical thermal control methods used for rovers. Thermal insulation will be provided by Aerogel to reduce heat loss at night when the outside temperatures are lowest. Other

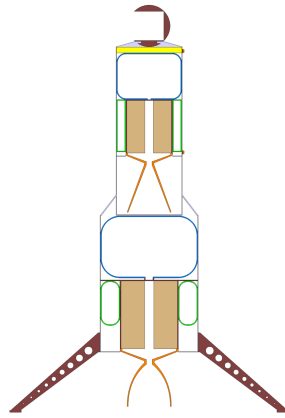


**Figure 26. Cross section of MAV.**

insulation materials considered during the decision process include MLI and Eccofoam. Aerogel was chosen for its high thermal conductivity and better performance in gaseous environments with dust.<sup>56</sup> In addition, a miniature loop heat pipe will act as a heat switch to transfer excess heat from equipment operating during the higher temperatures of daytime, and transfer heat to colder equipment at night. In comparison to other thermal switch systems that were considered, such as a mechanical heat switch and a mechanically pumped coolant loop, the passive loop heat pipe has a low mass, requires little electrical power, and has the capacity to transfer great amounts of heat over a long distance. The batteries, electronics, and any other mission-critical components that are sensitive to temperature fluctuations will be stored inside a warm electronics box, which will provide both thermal insulation as well as a structural enclosure to protect the equipment.<sup>57</sup>

#### D. Power

The MDV and MAV will use the same lithium ion batteries that the ITV utilizes. The MDV and MAV power requirements account for 3.4% and .5% of the total power requirements respectively, and therefore do not need an independent power source. The vehicle batteries will be charged via the solar panels on the ITV prior to separation, and the vehicles will function on that power for the duration of their missions.

## VI. Earth Re-entry Vehicle

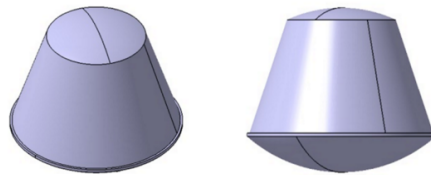


**Figure 27. Isographic and side views of the ERV CAD.**

The ERV system is designed to allow the sample cache to safely descend to the surface of the Earth. The ERV enters the atmosphere and brakes via drag, drogue chute, and parachute, bringing the sample to a sufficiently low velocity for safe landing and recovery.

**Table 24. Launch vehicle requirements and constraints.**

Technical Requirements	Affected Systems
Capable of integration with ITV	Structures System
Capable of containing and protection sample cache	All Vehicle Systems
Capable of surviving Earth atmospheric entry and landing	All Vehicle Systems

## A. Recovery

Two methods of recovering the sample were considered: docking with the ISS, and a direct-to-Earth landing. The selected choice is to return the sample to Earth directly, as docking with the ISS would require a large amount of excess  $\Delta V$ . The advantages of direct-to-Earth sample recovery include sooner requisition of the sample, and considerable fuel savings. Furthermore, every previous mission involving recovery from a foreign astronomical body has been performed through direct-to-Earth reentry. The science is already in place and has been used to return payloads much larger than the Martian sample being returned in this mission.

Docking with the ISS presents several challenges. Primarily, the returning ITV must enter the same orbit as the ISS in order to dock. This is more complex than regular reentry in terms of orbital dynamics, and it is calculated that the ITV would require an insertion burn to reach a  $\Delta V$  of 3.94 km/s in order to enter a 400 km orbit around Earth. The required maneuver could be handled by aerobraking in the Earth atmosphere, which would require extra time and additional heat shielding to protect the ITV. It is more time efficient to bring the sample directly to Earth, rather than spend extra time on more complicated orbital maneuvers to bring the ITV into the same orbit as the ISS. The ISS also has complicated docking procedures which would make the rendezvous and transfer of the sample cache difficult. Overall, ISS recovery would add a substantial amount of complexity to the mission.

## B. Contamination

Earth reentry also increases the risk of Earth contamination via the Martian sample, and vice-versa. As with any atmospheric reentry maneuver, a single failure in any number of systems will result in a mission failure.<sup>58</sup> The recovery of the sample must be performed in a way which highly reduces or eliminates the risk of back contamination from the Martian sample. Furthermore, in agreement with the European Science Foundation paper discussing safe sample return practices, upon its return to Earth the sample must be contained within a Biosafety Level 4 sample return facility.<sup>59</sup> This would require prior construction of such a facility before the sample is brought to Earth. To this end, the sample cache delivered to Earth will be placed within an airtight spherical container for the entirety of the mission, including the return trip and reentry. Until within the biosafety lab, the airtight container will prevent contaminants from entering or exiting the capsule. In addition, the ERV disperse the heat of reentry so as to avoid the destruction of the sample.<sup>60</sup>

## C. Vehicle Design

The capture method for transferring the spherical sample container from the MAV to the ITV requires the OS to be slid into the ERV through an opening in the backshell. Once the sample container has entered the ERV, it will slide into a holding apparatus and latching mechanism that will attach to the sample and ensure its safety throughout the rest of the mission. This design is shown in Fig. 28.

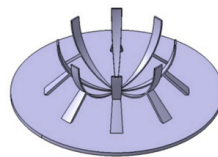


**Figure 28. CAD of ERV sample holding system.**

Earth sample recovery requires a dense heat shield for protection from the drag during reentry. The Apollo Command Module (ACM) was used as a rough framework for the ERV recovery plan, as few other references are available for returning planetary samples from other bodies. In this case, the ERV would be equipped with an ablative heat shield made of AVCOAT plastic, as well as supportive materials. The ERV has a maximum diameter of 0.9 m, while the heat shield has a volume of 0.023 m<sup>3</sup> and a mass of 60 kg. The vehicle is designed with a similar shape to the ACM, with a drag coefficient of 1.3.<sup>41</sup>

The ballistic coefficient of the ERV was used as the primary benchmark value to determine the feasibility of the ERV design as compared to similar missions. The ballistic coefficient of the ACM was within a range of 2500-5000 Pa.<sup>61</sup> Using the mass of the ERV and its widest-cross sectional area, as well as the determined drag coefficient, the ballistic coefficient was calculated to be 174 Pa. In comparison to the ACM, the ERV has a far smaller ballistic coefficient, and thus would dissipate more velocity during Earth reentry. Although a smaller ballistic coefficient would result in more drag, the speeds of reentry will be easily managed. The NASA

Stardust sample return capsule entered the atmosphere at roughly 13 km/s, and was successfully recovered for analysis. Furthermore, the Stardust sample return capsule diameter of 0.8 m is only marginally smaller than the ERV diameter, providing further support that safely landing the ERV capsule is feasible. The terminal velocity of the ERV at smaller heights above sea level was calculated to be just 53 m/s, which is easily manageable using conventional parachutes and drag.

The ERV will be brought down from its initial velocity of 11 km/s to an acceptable landing speed using the drag of the atmosphere until a height of 33.5 km. At this height a drogue parachute will deploy, followed by the final parachute at an altitude of 3.5 km. The ERV will land in Utah, similar to the Stardust mission.<sup>62</sup>

## VII. Radiation

During the long journey to and from the Martian surface, the main concern for radiation protection would be particles coming from galactic cosmic rays, which mainly consist of protons and heavier ions that can break atoms apart on any surface they come in contact with. As research shows, Curiosity measured radiation equal to 300 mSv in a 6 month span on Mars.

The sample can be protected through two methods of radiation protection. The first involves surrounding the object with a magnetic field, which requires an unsustainable amount of power. Although research is currently being conducted for future missions on how to create such a field with lower power requirements, this type of technology would not be approved for flight by a launch window of 2020.<sup>63</sup> The second method, involving surrounding important equipment and the sample with radiation resistant material, proves more feasible. Two types of radiation resistant material were researched for possible application to the MSRS. The possibility of using hydrogenated boron nitride nanotubes was considered. There is currently research being conducted on this material for application in deep space missions.<sup>63,64</sup> Solar flares are high energy protons which account for only 5% of the radiation that will be experienced. In comparison, galactic cosmic rays, which lack electrons, allow themselves to become radioactive when an object hits the rays and draws electrons away from that object. It is these protons and ions found in the GCR and the solar flares that make radiation protection essential in the MSRS design. Polyethylene, which contains hydrogen and is currently used in ISS crew quarters to shield from harmful rays, is a possibility for radiation shielding, yet lacks structural support.<sup>65</sup> Hydrogenated boron nitride combines both strong structural support and radiation protection. This material can be made into thin fibers and then woven together to create a supportive and safe material. This technology holds potential for shielding future manned missions from harmful radiation.<sup>64</sup> With a TRL of 6, hydrogenated boron nitride can be developed into a safe and reliable technology for the mission.

## VIII. Communications

Communication between planetary bodies presents several complications that must be addressed by the chosen communication system. Traveling at light-speed, communication between Earth and the ITV would take at least several minutes, requiring any transmissions between the two planets to carry as much information as possible and limit data loss. The mission also requires effective communication between the MAV on Mars and the ITV in orbit.

For communication between the MAV and the ITV, Ka-band technology was selected as the best option. Between Ku and Ka band frequencies, Ka frequencies require smaller antennae to function with the same level of efficiency.<sup>66</sup> For an antenna set on the MAV, a smaller antenna would reduce mass requirements. For communication between the ITV and Earth, X-band technology was selected. Most communication to and from space currently uses Ku-band technology, or some Ka-band technology. Therefore, there is interest in freeing up some frequencies of bandwidth allocation in order for communications to continue running smoothly and without interference. This pushed the decision to use X-band technology for communication, as introducing another Ku or Ka frequency to the already crowded bandwidth would introduce risks of signal overlap or loss. Furthermore, because X-band technology works at 7-8 GHz frequencies, it is less susceptible to rain fade than Ku and Ka bands. X-band signals also maximize data transfer when compared to other frequencies out of the same sized antenna.<sup>67</sup> The use of optical communication technology was considered for the mission, but was discarded due to a lack of development. The ITV would be able to send transmissions to orbiting satellites around Earth, which would then be transferred to the ground, thereby avoiding the dangers of rain fade and other weather-obstacles. For the sake of a successful mission, proven technology was chosen in order to improve the reliability of the communication system. In addition, unavoidable risk

to mission communication is the threat of sun blackout, which would occur when Mars and the Earth are on opposing sides of the Sun. In this case, communication would be disrupted, and therefore it is important that the ITV reaches Mars before such an event occurs.<sup>68</sup>

Both the ITV and the MAV will use dish antennae, as they are durable, affordable, and well suited for deep space missions.<sup>69</sup> The ITV and MAV will both be given lower-gain antennae for redundancy and emergency purposes. The orientation of the ITV relative to the Earth will constantly be changing during the transit trip to and from Mars, and therefore the main antenna will be oriented to always face the back of the spacecraft. Using a gimbal system similar to that of the Mars Reconnaissance Orbiter (MRO), the antenna will be consistently pointed toward Earth for the duration of the mission.<sup>70</sup> The redundant low-gain antenna has a much wider field of transmission, allowing the Deep Space Network on Earth to pick up the signal regardless of the orientation of the spacecraft.<sup>71</sup>

## IX. Mission Process

The launch vehicle and the movement of the sample cache are integral components of the mission. Trade studies were conducted on these systems to determine the method that provides the lowest cost, mass, and complexity, while maintaining the capability of integrating with the rest of the MSRS.

### A. Launch

The launch vehicle must transport the entire system into LEO and set up the initial burn towards Mars. Launch will occur from an established spaceport and in time for the specified orbital transfer outlined previously. The launch vehicle is largely dependent on the mass of the total system. Secondary factors include the fairing size, availability, cost, and reliability. Fairing size also puts constraints on the structure of the MSRS. Due to the relatively low mass of the MSRS, it would be far more advantageous for the launch vehicle to send the ITV into the Mars transfer orbit, rather than expending the ion engines of the ITV. With the launch vehicle performing the injection, propellant is reduced by 75%, and the mission is able to launch a year later, giving an extra year of testing and development.

**Table 25. Launch vehicle requirements and constraints.**

Technical Requirements	Affected Systems
Capable of lifting MSRS mass	Rocket Thrust
Capable of providing Launch C <sub>3</sub> of 14 km <sup>2</sup> /s <sup>2</sup>	Rocket Thrust and Size
Capable of Launching entire MSRS in single launch	Fairing Size

#### 1. Launch Vehicle Selection

For a total mission mass of 3060 kg, a handful of options are available to launch the vehicle, including the Atlas 5, the Falcon 9 FT, and the Delta 4 M+ (4,2). These vehicles all offer a C<sub>3</sub> of 14 km<sup>2</sup>/s<sup>2</sup> and are launched from US sites. Vehicles such as the Delta 2 and Ariane 5 were not considered since they either have too little payload capacity, too excessive payload capacity, or require international cooperation.<sup>72</sup>

The Atlas 5 launched the MSL in 2011 and has a sizable history of launching interplanetary craft. The vehicle is produced by United Launch Alliance and has a 100% success rating. The mission parameters require a 500 model of the Atlas 5, which is a bit smaller in launch volume than the 400 models. The Falcon 9 FT is the newcomer in launch vehicles, run by commercial space pioneer Space Exploration Technology. The Falcon 9 FT is the third iteration of the Falcon 9 launch vehicle, and the only iteration that is powerful enough to reach the desired C for the planned MSR mission. The Falcon 9 FT has the shortest track record of the three launch vehicles, with only three launches as of April 2016. The Falcon 9 family has had one failure in 23 total launches, though it was not an FT that suffered the failure. The Delta 4 M+ (4,2) is the member of the Delta 4 family that is most optimal for the MSRS. This launch vehicle has more than twice as many launches as any of the previous options. The Delta 4 is also a part of the United Launch Alliance and has a 100% success rate. It is most advantageous to use the Delta 4 M+ (4,2) as the launch vehicle, as it has the most accurate parameters, a reasonable cost, and the highest probability of success.<sup>72</sup>

## 2. Effects on Mission Systems

The Delta 4 M+ (4,2) has specific payload requirements that need to be met by the MSRS. The vehicle has a fairing that is 4 m in diameter and 6.9 m in payload encapsulation length, with an additional 4.5 m in the conical section. All mission systems must be able to fit or retract into these dimensions for launch. Analysis on structures confirms that the entire MSRS will be able to fit inside the fairing.<sup>72</sup>

### B. Sample Transfer and Rendezvous

The rendezvous and capture of the OS presents unique challenges. Not only is the OS a small, non-cooperative target that the ITV must locate and capture, but a majority of current Automated Rendezvous and Capture (AR&C) technology is calibrated to for a LEO environment. However, space agencies have become adept at autonomous rendezvous and, using standardized methods coupled with past mission experiences and heritage technologies, the requirements for rendezvous and capture are achievable.

**Table 26. Summary of the requirements for rendezvous.**

Technical Requirements	Affected Systems
Fully autonomous rendezvous	GN&C, RCS
Capable of detecting unpowered OS	Hardware
Compatible with MAV design	Hardware
Mechanism for transferring OS to ERV	Hardware

#### 1. Preliminary Analysis

The first step in developing a rendezvous strategy for the mission was selecting a baseline procedure from the standardized methods used in past missions. Currently, two methods have been employed by space agencies for rendezvous: (1) the Stable Orbit Rendezvous (SOR); and (2) the double co-elliptic rendezvous. SOR was immediately eliminated from consideration because it is designed for vehicles with long range radar systems, which only the Space Shuttle is capable of carrying.<sup>73</sup>

Co-elliptic rendezvous has been used for several other NASA missions, and was also selected for use by the Orion Capsule. This rendezvous strategy will place the ITV in a lower co-elliptic orbit, an orbit that has a difference in semi-major axis height ( $\Delta H$ ) between the perigees of the two orbits equal to the  $\Delta H$  between the apogees of the two orbits. The ITV then performs a number of Hohmann raises to reach the OS.<sup>74,75</sup>

#### 2. Detailed Design

There are a number of different configurations that can change the rendezvous and capture profile. A summary of the different configurations is provided in Table 27.

**Table 27. Possible rendezvous profile configurations.**

Parameter	Possible Configurations
Capture method	Free orbiting OS, Docking with MAV upper stage
Number of Hohmann raises	1, 2, 3
Number of hold points	1, 2, 3

One of the primary decisions that had to be determined was whether capture should be conducted with a free-flying OS, or with the sample container still attached to the second stage of the MAV. This decision would also have to be compatible with the ITV design. Capturing a free-flying OS would allow for the development of a much simpler capture mechanism, as orientation of a spherical OS would not matter and the risk of collision is less severe. However, locating the OS would be difficult due to its small size. Furthermore, the OS would be almost non-cooperative with the exception of an Ultra High Frequency (UHF) Beacon that would provide little information for the ITV. On the other hand, retrieving the sample from the second stage of the MAV may make location simpler. The MAV second stage could be designed with a wider range of

communications systems to allow the MAV to cooperate with the ITV as it conducts rendezvous. However, this would add more mass to the MAV due to the need for additional propellant to conduct minor maneuvers, and would require that more stringent docking procedures be enforced.

The number of Hohmann raises that the ITV conducts to reach the MAV also deserved some consideration. Using more Hohmann raises provides more passive safety and allows mission control to further monitor the progress of the ITV; however, it adds additional complexity to the mission and prolongs the process. The number of hold points also had to be determined. Hold points are points during the rendezvous where the ITV will conduct station keeping maneuvers until mission control can verify that rendezvous is going as planned. Increasing the number of hold points would allow for better monitoring of the rendezvous process. However, it would also increase the complexity and require more maneuvers from the ITV.

In order to simplify the capture process and the design of the ITV and MAV, it was determined that the sample container would be released by the MAV in orbit and picked up by the ITV. The number of hold points was fixed to just one before the MAV initiates proximity operations. Mission control can actively monitor the ITV during the co-elliptic drifts between the Hohmann raises, and initiating hold points would only unnecessarily complicate the procedure. A hold point on the MAV V-bar allows mission control to determine if conditions are suitable for the MAV to release the OS and the ITV to make its approach.

The MAV rendezvous operations will be performed similarly to a process proposed by a team at TRW Space and Electronics. The MAV will launch into a 500 km orbit, as specified in the MAV design section, while the ITV orbits 20 km below and 75 km downrange. Constant communication will be maintained between the second stage of the MAV and the ITV, and once the ITV acquires visual of the MAV second stage, the rendezvous operations will begin. The ITV will conduct two Hohmann raises. The second Hohmann raise will place the ITV about 200 m in front of the MAV.<sup>76</sup> Once mission control determines the rendezvous is operating without any anomalies, the ITV will initiate proximity operations.

**Table 28. Summary of ITV rendezvous operations.**

Segment	Description	Altitude Change (km)
1	Coelliptic Drift	0
2	Hohmann Raise	10
3	Coelliptic Drift	0
4	Hohmann Raise	10
5	Hold Point	0

Both the MAV and the ITV will have to orient themselves. The MAV will orient along the velocity vector, or V-bar, direction while the ITV will orient along the negative V-bar direction. Once that is complete, the ITV will make a simple V-bar approach. The MAV will release the OS once the ITV has reached a relative distance of 50 m and the MAV will deorbit. The ITV will then complete the V-bar approach. The ITV is designed with a funnel that guides the OS to the back opening of the ERV. Once the OS is safely in place, mechanical latches will seal the OS into the ERV.

### 3. Hardware

In order for the ITV to complete AR&C, it will need to measure the range, range-rates, line-of-sight direction, relative attitude, and angular rate of the OS. Some of the hardware necessary to make these measurements include star tracker suites, accelerometers, and gyros, which will be present and used throughout the mission. Two additional pieces of hardware are key for AR&C: optical navigation (OpNAV) systems and light detection and ranging cameras (LiDAR). Both the OpNAV and the LiDAR will need to be capable of taking measurements from thousands of kilometers away.

The OpNav system on the MRO was the first device considered for the ITV. OpNav used a comparison of the predicted location of the two Martian moons with observations from onboard camera observations for navigation. OpNav is a flight proven technology and is already calibrated to a Martian environment. This technology can be used to both navigate for rendezvous and more accurately navigate during entry. Another piece of equipment considered from the MRO mission was a modified version of the High Resolution Imaging Science Experiment (HiRISE). Some additions would need to be made in order for HiRISE to provide navigation. For the LiDAR system, a new piece of technology, Sensor Test for Orion RelNav Risk Mitigation,

was considered. This is a Visual navigation system (VNS) that uses LiDAR for accurate determination of range and velocities.<sup>77</sup> This would provide redundant visual of the OS during the capture process. Another possible option considered was the Boeing Vision-based software for Track, Attitude, and Ranging (Vis-STAR). Vis-STAR can process visible or infrared camera images, providing coverage regardless of light, range, or background conditions.<sup>75</sup> In addition, it was used by NextSat during the Orbital Express (OE) missions. Finally, the Advanced Video Guidance Sensor (AVGS) was used by both DART and OE, which makes it an ideal candidate for consideration. OE was a technology demonstration mission to determine the feasibility of AR&C of an uncooperative satellite. It conducted a number of precise AR&C operations that are comparative to the precision required during this mission.

The AVGS and the MRO OpNav were decided upon for the navigation of the ITV during rendezvous. AVGS was used on the OE missions, which demanded incredibly precise measurements. Similar precision would be necessary during the MSR rendezvous. The MRO OpNav was chosen because it is a heritage technology that is already calibrated to the environment of Mars. This reduces complexity, as a whole new system would not have to be developed to meet the requirements.

## X. Vehicle Health Monitoring and Contingency Planning

An MSR mission has never been attempted, and several components of the mission involve new technologies that are being demonstrated simultaneously. The complexity and novelty of the MSRS poses several opportunities for failure. For this reason, it is important that plans are in place to deal with any emergency situations and assess the damage caused by any problems that occur. The requirements for vehicle health management were generated by assessing which systems and processes are most vital to the success of the mission. These components of the MSRS will require methods of monitoring their operations and measuring their performance in order to ensure continued functionality. In the event of a system failure or malfunction, failure phases will be presented, and the effect of each failure scenario on the overall mission will be discussed.

The goal of assessing the issues most likely to occur is to determine the potential of salvaging the mission, and to establish a protocol for each situation. Every factor of a failure is measured against mission success criteria. Complete mission success is defined as returning the sample cache safely and without contamination from Mars to Earth. Mission failure is defined as failing to transport the sample to Earth.

### A. Vital Systems Analysis

To begin the design of the health monitoring system, several mission components were analyzed to determine their criteria for continued functionality. These components were selected based on their role in the mission and the possibility that, depending on the level of failure, they could cause an overall mission failure. The integrity of these systems will determine the outcome of the mission, and therefore it is critical that any associated health factors are monitored.

**Table 29. Vital mission components and associated health factors.**

System/Processes	Vital Health Factors
Engine	Pressure, Temperature, Flow Speed
Electrical Systems	Radiation Absorption, Temperature, Voltage Levels, Current Levels
Propellant Tanks	Pressure, Temperature, Strain
Mars Descent	G force, Temperature, Altitude, Geographic Location, Orientation
MAV	Orientation, Temperature, Radiation, Sample Acquisition
Mars Launch	G force, Temperature, Altitude, Dynamic Pressure
MAV/ITV Rendezvous	Sample Acquisition, Orientation, Approach Distance
Earth Entry	G force, Temperature
Sample Safety	Temperature, Radiation



## B. System Monitoring

The monitoring mechanisms chosen for implementation within the vehicle designs are matched to specific system health factors that affect the functionality of the mission components specified above. Table 30 outlines the important health factors and the devices that could be used to monitor each factor.

**Table 30. Health factors and associated mechanism for measurement and monitoring.**

Health Factor	Measurement Mechanism
Temperature	Thermocouple
Pressure	Pressure Gage
Flow Speed	Flowmeter
Radiation Absorption	Radiometer, Roentgenometer
Strain	Strain Gage
Voltage Levels	Voltmeter
Current Levels	Ammeter
G Force	Accelerometer
Altitude and Approach Distance	Camera, Radar
Geographic Location	Camera
Orientation	Gyroscope, Star Tracker
Sample Acquisition	Photoelectric Sensor, Camera

Beyond monitoring the health of all vital systems, computing systems must be able to tell when a health characteristic is outside of the normal range. To assess the overall health of each system, a red line analysis methodology will be used in which factors are defined as nominal until they move outside the red line region. If this health factor remains outside the nominal range, the system is assumed to have failed. This analysis can be performed by on-board computers automatically. These red line regions will be defined by ground testing within environments comparable to what will be experienced by each component during the mission.

## C. Failure Modes

Due to the novelty of many elements of the MSRS, there exist numerous failure modes that need to be investigated to determine protocol during emergencies. The possible failure modes are investigated by each individual vehicle and then classified as mission saved, mission salvageable, or mission failed. For a mission to be qualified as saved, the MSRS must be able to complete the mission despite the system failure. To be classified as potentially salvageable, the MSRS must be capable of achieving a stable orbit around Earth where the sample cache can potentially be recovered, and then returned to Earth using another vehicle. Mission failure encompasses any fail mode in which the sample does not return to Earth and any potential recovery of the sample using an additional vehicle is deemed unrealistic.

The first vehicle failure modes considered were for the ITV, which fall into two main categories: propulsion failure or electrical failure. Propulsion failure for the ITV can occur in multiple configurations that can change the outcome of the mission significantly. If only one engine fails then the mission can proceed, because the ITV possess two engines for redundancy. Thus, the mission outcome would be classified as mission saved. On the other hand, if both engines fail before the Earth transfer is complete, then the mission would be categorized as mission failed. If the engines fail after the ITV has completed the Earth transfer, then the mission is categorized as potentially salvageable, as a vehicle could possibly rendezvous with the ITV and retrieve the sample. In the case of ITV electrical failures, the outcome is almost always mission failed. The ITV position would be relatively unknown in any case, and the possibility of retrieving the sample from the ITV would be slim. The next vehicle considered was the MAV, which represents the element of the mission with the highest risk, and therefore has a multitude of possible fail states that result in mission failed. If the MAV propulsion systems fail and the MAV is unable to ascend to the proper orbit, then the sample will be unretrievable, resulting in mission failure. If the MAV electrical systems fail, then once again the MAV will be unable to ascend to a proper orbit, resulting in mission failure. If the MAV orientation is shifted in a direction that does not permit a safe launch, then the mission will fail. The final vehicle fail state analysis

is for the ERV. The ERV could fail to deploy as the ITV passes over Earth. The ITV could likely maneuver into a stable orbit around Earth, classifying the mission as potentially salvageable, since another vehicle could be launched to retrieve the sample. If the ERV experiences a catastrophic failure during entry, the mission will likely fail due to contamination and possible destruction of the sample. Additionally, if the OS container leaks, or the climate control systems fail, then the mission would be categorized as mission failed due to the contamination or destruction of the sample.

## XI. Cost

The following section provides a cost estimate to analyze the economic viability for Project Argonaut. As the project is still in the preliminary phase of design, the cost may change later on in development depending on the status of the space industry and the TRL of the technology used onboard.

### A. Cost Estimation Methods

The cost of the mission is dependent on multiple variables including the size, complexity, technological innovation, and design life of the vehicle. It is also a function of risk tolerance, methods for reducing risk, management style, documentation requirements, project-management controls and the size of the performing organizations. Due to the high cost of such a mission, a proper cost analysis is critical in determining the feasibility of the mission as an overly high cost mission will not be considered due to the economic constraints of the company and industry. There are three basic methods used in the industry to derive the cost: detailed bottom-up estimation, analogy-based estimation, and parametric estimation.

Detailed bottom-up estimation incorporates the analysis done on each subsystem, including the cost of each material used and the labor to develop and produce each system. The method can be tailored to specific missions, especially ones that are newly designed and different from existing missions. However, the method is very time consuming and requires thorough documentation. All of these values would be documented by the lead engineers of each department during the manufacturing process, which will not be available in the preliminary design phase. Therefore, the method is primarily used in the production phase, after the design is finalized with a majority of the technical uncertainties resolved during the development.

Analogy-based estimation utilizes data from existing missions and adjusts the cost from similar missions to formulate an estimation. The method can be applied during any phase of design; however, it provides a lower accuracy compared to the detailed bottom-up method. An analogous mission with similar technology and requirements has to exist for the method to be used. Unfortunately, no historical mission is similar to the description in the RFP, making the method impractical for cost estimates for Project Argonaut.

The last method is parametric estimation, which employs mathematical relationships, Cost Estimating Relationships (CER), between cost and known physical, technical, and performance parameters. The method is a top-down approach where only the system requirements and top-level design specifications are required. Since the approach utilizes historical trends, the estimated cost for the mission will not be completely accurate due to technological advancement over time. Therefore, more parameters are incorporated into the CER including the skill levels of contractor engineers and technicians, occurrence of unforeseen technical problems, business base of all contractors involved, requirements changes, and test failures in order to get a more precise cost value.<sup>78</sup>

### B. Results

The total cost for the project is estimated to be \$4.2 to \$6.5 billion depending on the level of difficulty of the technology onboard. As the mission will demonstrate new technology for future missions, it is considered to be of high or very high difficulty. The cost was estimated using a parametric estimate with the Advanced Method Cost Model (AMCM).<sup>79</sup> The cost estimate was compared to estimates from other organizations for the same mission with similar programs, which can be seen in Table 31. The values are relatively similar to the cost range estimated for Project Argonaut.

**Table 31. Cost comparison from different organizations.**<sup>79–82</sup>

Organization/Source	Launch Year	Total Cost (\$B)
FAS	2020	4.2 - 6.5
NASA 2009	2015	3.6
		4.5
		3.5
NASA 2010	2015	2.5
	2024	3.1
Mars Exploration Program Analysis Group	2020	5

## XII. Conclusion

This concludes the design proposal for the MSRS of Project Argonaut. The mission profile defined in the RFP demands a design that is innovative, yet feasible and cost effective. This proposal provides several plausible solutions to obstacles associated with MSR missions, and presents reasonable justification for the validity of each design decision. Furthermore, this proposal explores concepts that distinguish it from other proposed MSR missions. The chosen architecture of the MSRS for Project Argonaut is designed to provide flexibility within the mission time frame, in order to increase the feasibility and salvageability of the mission. The time frame of the mission is flexible in that it consists of a single launch, eliminating the need to coordinate multiple launches within the launch window. The MAV is also capable of surviving on the Martian surface for an extended period of time, through the use of hybrid propulsion technologies. These design decisions provide a larger number of options in case of a failure in the key stages outlined in the mission concept section. Additionally, Project Argonaut utilizes multiple new technologies that push the boundary of current space development. The MSRS will serve as a testing bed for innovations that will be integral to the advancement of space technology towards manned missions to Mars, as an MSR mission does not pose an immediate threat to human life. The inclusion of interplanetary ion propulsion, inflatable heat shield descent, and hybrid MAV propulsion in the design of Project Argonaut presents this mission as a stepping stone towards the future of space exploration.

## Acknowledgments

Team Argonaut would like to thank Professors Micheal Grant and Kathleen Howell as well as Graduate Student Ash Das for their support and input on this proposal.

## Appendix

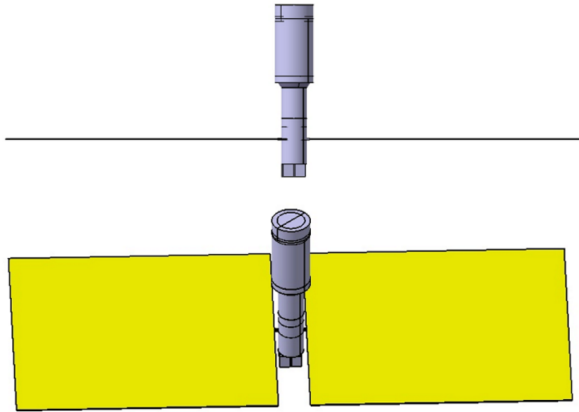


Figure 29. Views of the ITV CAD model with solar panels deployed and retracted.

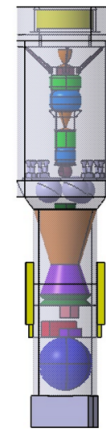


Figure 30. Side view of MSRS assembly.

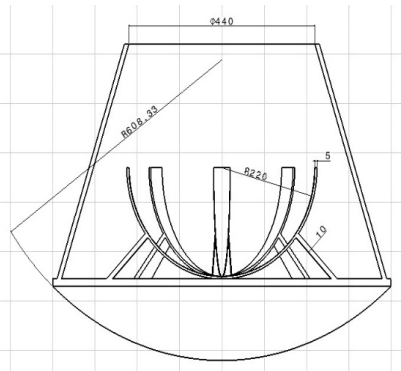


Figure 31. Technical dimensions of ERV model.

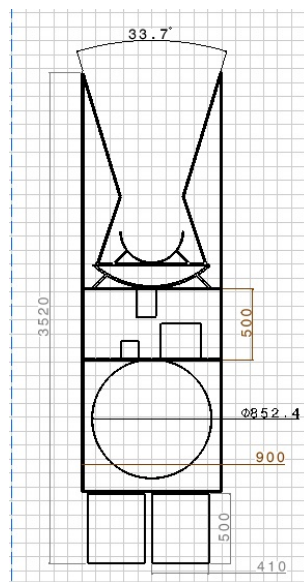


Figure 32. Technical dimensions of ITV model.

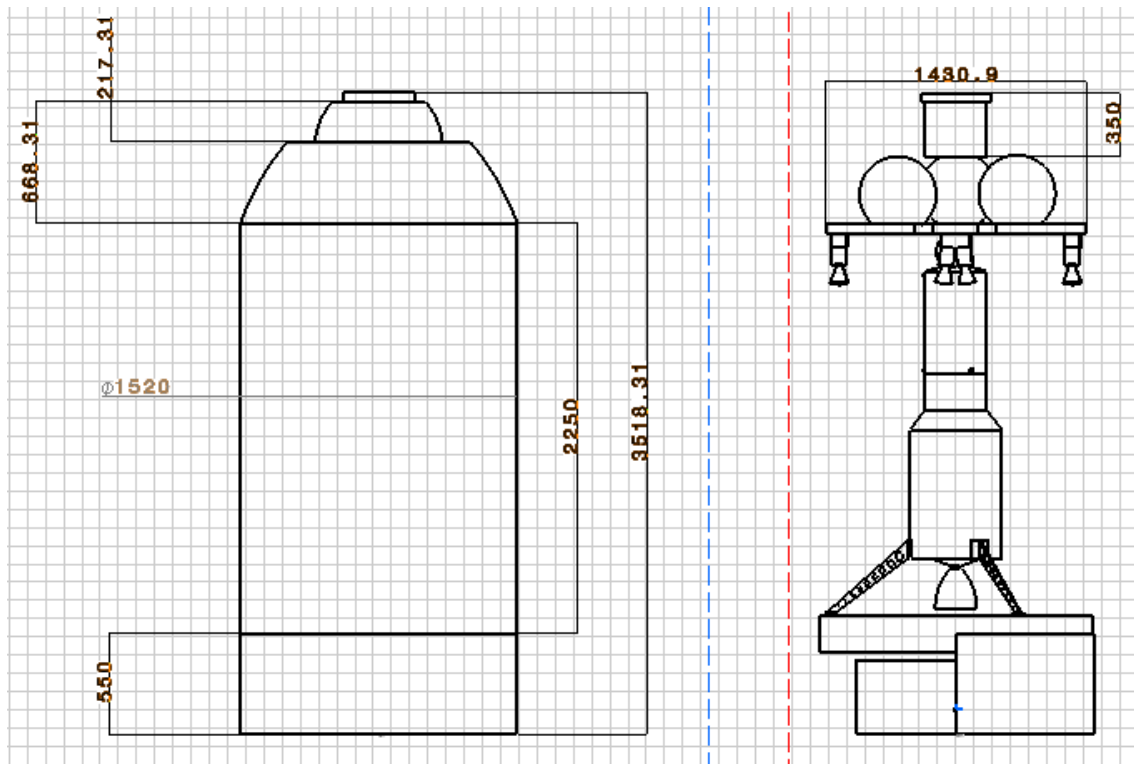


Figure 33. Technical dimensions of MDV model.

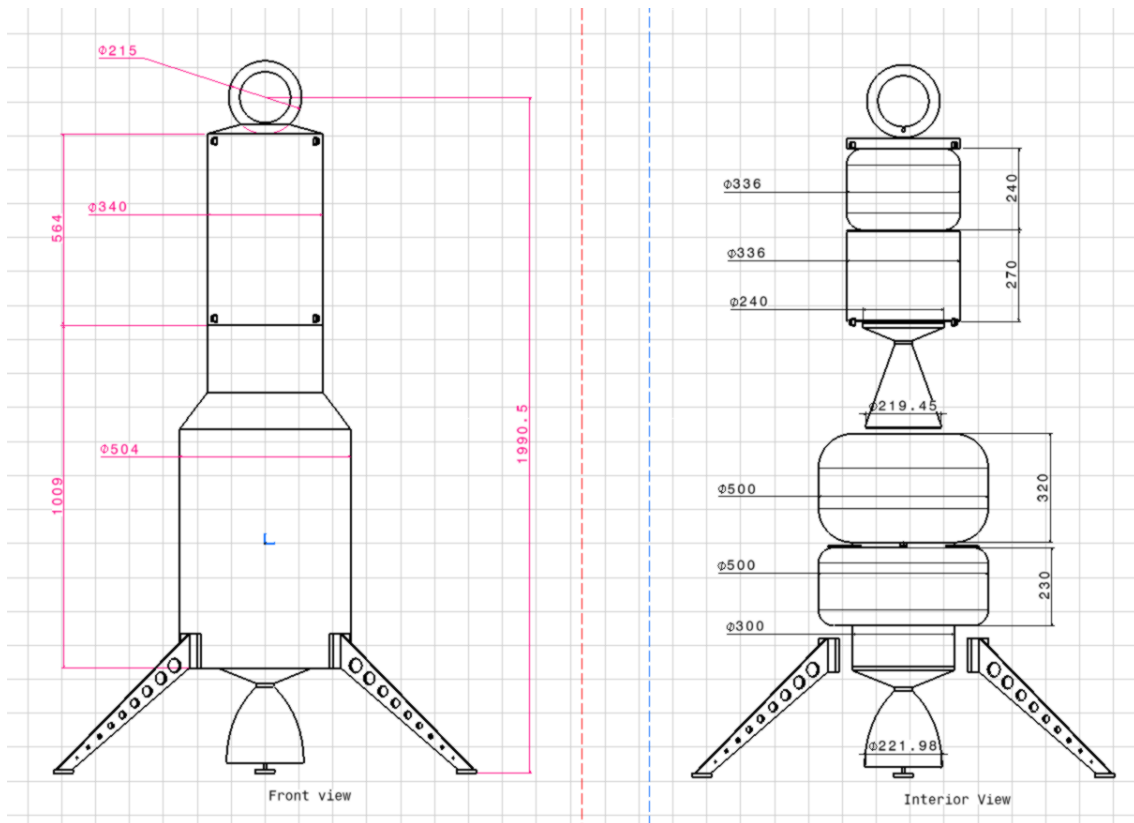


Figure 34. Technical dimensions of MAV model.

Table 32. Power requirement breakdown by system.

System	Component	Power (W)
Propulsion	Downrated HiPEP	24400
Mars Descent	Thermal Control	10
	Propulsion	44
	Attitude Control	478
	Command & Data	4
	Communications	307
Mars Ascent	Power	82
	Thermal Control	10
	Attitude Control	6.3
	Command & Data	2.6
Power Dist.	Communications	57.2
	Power	48.3
Power Dist.	---	1,781.5
<b>MSRS</b>	<b>Total</b>	<b>27230.89</b>

Table 33. Mass requirement breakdown by system.

System	Subsystem	Component	Mass (kg)
ITV	Engine	HiPEP (2)	886
		Propellant	Xenon
	Tanks	Hydrazine	50
		Xenon Tanks	13
	Structures	Hydrazine Tanks	4
		Insulation	13
		Fairing	58
		Avionics	172
		Wiring	53
	Attitude Control	Heatsield	75
ACS		37	
Power Systems	RCS	14	
	Solar Arrays	183.4	
<i>Total mass</i>	Batteries	111.5	
		<b>2152.9</b>	
Mars System	MDV	Structures	120
		Heat Shield	20
		Parachutes	50
		Sky Crane	214
		Propellant	120
	MAV	<i>Total mass</i>	<b>524</b>
		Structures	49
		Other Systems	33
		Propellant	188.4
		Payload	3
<i>Total mass</i>	Base System	15	
		<b>288.4</b>	
<i>Total mass</i>		<b>812.4</b>	
Earth System	ERV	Heat Shield	60
		Structures	35
		Payload	5
	<i>Total mass</i>	<b>100</b>	
<b>MSRS</b>	<b>Total Mass</b>	<b>3060.3</b>	
Launch Vehicle	Delta M+(4,2)	323000	
	<b>Launch Mass</b>	<b>326060.3</b>	

Table 34. Morphological chart of all design solutions.

Morphological Chart									
System	Component	Subcomponent	Option 1	Option 2	Option 3	Option 4	Option 5	Option 6	
Launch	Vehicle	—	Atlas V	Delta Heavy	Delta III(5.4)	Delta III(4.2)	Falcon 9		
		Trans-Earth Injection	Electric Propulsion	Chemical Propulsion					
		Trans-Mars Injection	Electric Propulsion	Chemical Propulsion					
System Dynamics	Orbits	Mars Orbital Insertion	Powered	Aerocapture					
		Number of Launches	1	2	3				
		Chemical Ion	RL-10A-4-2	RL-10B-2	Merlin 1-D	J-2X	RL60		
ITV	Propulsion	Final Engine Selection	NSTAR	HPEP	NEXT	Boeing 601HP	Boeing 702		
		Material	RL-10B-2	HPEP	Downrated HPEP				
		Descent Method	6081-T6 Aluminum	7075-T6 Aluminum	R569400 Titanium				Supersonic Retro Propulsion
MAV	Structure	—	Parachute	H/AD	Skycrane	Airbags	Balloon		
		Main Engine Propellant	Bi-liquid	Liquid and Solid	Solid	Gel			
		Number of Stages	1	2					
ERV	Thermal	ACS	Thrust Vector Control Gimbaling	Liquid RCS	Hybrid RCS				
		Insulation	Rigid Aeroshell	Skeleton	Rigid Tank Bodies	Warm Electronics Box	Igloo		
		Heat Switch	Aerogel	Multi-layer Insulation	Ecofoam				
MSRS	Power	Battery Type	Mechanical Heat Switch	Miniature Loop Heat Pipe	Mechanically Pumped Coolant Loop				
		Recovery Location	AgZn	NIcA	NIH2	Lilou			
		Radiation	ISS	Earth					
MSRS	Power	—	Electromagnetic Fields	Polyethylene	Hydrogenated Boron Nitride Nanotubes				
		Power Source	Solar Panels	RTGs	Fuel Cells				
		Solar Array Type	Ultraflex	SLASR					
MSRS	Power	Battery Type	AgZn	NIcA	NIH2	Lilou			
		Distribution System	DET	PPT					
		Communications	Frequency Range	Ku-Band	Ka-Band				

## References

- <sup>1</sup>"Delta IV Payload Planners Guide," United Launch Alliance Rept. 06H0233, Sept. 2007, <https://www.apsu.edu/sites/apsu.edu/files/astronomy/DeltaIVPayloadPlannersGuide2007.pdf> [retrieved 14 April 2016].
- <sup>2</sup>"Ion Propulsion: Farther, Faster, Cheaper," *Glenn Research Center* [online], [http://www.nasa.gov/centers/glenn/technology/Ion\\_Propulsion1.html](http://www.nasa.gov/centers/glenn/technology/Ion_Propulsion1.html) [retrieved 24 Mar. 2016].
- <sup>3</sup>Morring, F., "NASA's J-2X Engine To Be Mothballed After Testing," *AviationWeek* [online], <http://awin.aviationweek.com/ArticlesStory/tabid/975/Status/IPAddress/id/62c35e3e-0c9e-40e7-86dd-61052f491f27/Default.aspx> [retrieved 31 Mar. 2016].
- <sup>4</sup>Wade, M., "Nuclear/LH2," *Encyclopedia Astronautica* [online]. <http://www.astronautix.com/props/nucarlh2.htm> [retrieved 19 April, 2016].
- <sup>5</sup>Bennett, G. L., "Nuclear Thermal Propulsion," NASA N91-28216, June 1990.
- <sup>6</sup>Oleson, S. R., "Electric Propulsion Technology Development for the Jupiter Icy Moons Orbiter Project," NASA, 2004.
- <sup>7</sup>"Frequent Asked Questions about Ion Propulsion," *Jet Propulsion Laboratory* [online], <http://nmp.jpl.nasa.gov/ds1/tech/ionpropfaq.html> [retrieved 10 Nov. 2015].
- <sup>8</sup>"DAWN," *Jet Propulsion Laboratory* [online], <http://dawn.jpl.nasa.gov/technology/> [retrieved 10 Nov. 2015].
- <sup>9</sup>Foster, J. E., Haag, T., and Patterson, M., "The High Power Electric Propulsion (HiPEP) Ion Thruster," NASA, Sep. 2004.
- <sup>10</sup>Clark, S., "Boeing's first two all-electric satellites ready for launch," *Spaceflight Now* [online], <http://spaceflightnow.com/2015/03/01/boeings-first-two-all-electric-satellites-ready-for-launch/> [retrieved 20 Nov. 2015].
- <sup>11</sup>"Propulsion System," *MANTIS Corporation* [online], [http://www.propagation.gatech.edu/ECE6390/project/Fall2010/Projects/group10/MANTIS\\_2010\\_SatCom/MANTIS\\_2010\\_SatCom/PropulsionSys/default.html](http://www.propagation.gatech.edu/ECE6390/project/Fall2010/Projects/group10/MANTIS_2010_SatCom/MANTIS_2010_SatCom/PropulsionSys/default.html) [retrieved 12 Feb. 2016].
- <sup>12</sup>Patterson, M. J., Pinero, L., and Sovey, J. S., "Near-Term High Power Ion Propulsion Options for Earth-Orbital Applications," AIAA, Aug. 2009.
- <sup>13</sup>Rayman, M. D., Fraschetti, T. C., Raymond, C. A., and Russell, C. R., "Dawn: A mission in development for exploration of main belt asteroids Vesta and Ceres," *Acta Astronautica*, April 2006.
- <sup>14</sup>Alcoa, "Alloy 7075 Plate and Sheet," *Alcoa Mill Products* [online], [http://www.alcoa.com/mill\\_products/catalog/pdf/alloy7075techsheet.pdf](http://www.alcoa.com/mill_products/catalog/pdf/alloy7075techsheet.pdf) [retrieved 19 April 2016].
- <sup>15</sup>Titanium Engineers, "Titanium 6AL-4V Ti 6-4 / Grade 5 (UNS R56400)," [online], [http://www.offshore-europe.co.uk/\\_novadocuments/70982?v=635574471464900000](http://www.offshore-europe.co.uk/_novadocuments/70982?v=635574471464900000) [retrieved 19 April 2016].
- <sup>16</sup>"Multi Layer Insulation Films," *DUNMORE* [online], <https://www.dunmore.com/products/multi-layer-films.html> [retrieved 10 Nov. 2015].
- <sup>17</sup>Doody, D., "Chapter 11. Typical Onboard Systems," *Jet Propulsion Laboratory* [online], <https://solarsystem.nasa.gov/basics/bsf11-4.php> [retrieved 20 Jan. 2016].
- <sup>18</sup>Doody, D., "Thermal Control Subsystem," *Deep Space Craft: An Overview of Interplanetary Flight*, Chichester, UK, 2010, pp. 168-169.
- <sup>19</sup>Larson, W. J., and Wertz, J. R., "Spacecraft Subsystem: Thermal," *Space Mission Analysis and Design*, 3rd ed., El Segundo, CA, 1999, pp. 428-458.
- <sup>20</sup>Miller, D., and Keese, J., "Spacecraft Power Systems," MIT Open Courseware, 16.851 Satellite Engineering, Fall 2003.
- <sup>21</sup>Zona, Kathleen, "Fuel Cells: A Better Energy Source for Earth and Space," *NASA Glenn Research Center* [online]. [http://www.nasa.gov/centers/glenn/technology/fuel\\_cells.html](http://www.nasa.gov/centers/glenn/technology/fuel_cells.html). [retrieved 20 Jan. 2016].
- <sup>22</sup>Piszczor, M. F., Jr., O'Neill, M. J., Eskenazi, M. I., and Brandhorst, H. W., Jr., "The Stretched Lens Array SquareRigger (SLASR) for Space Power," *4th International Energy Conversion Engineering Conference (IECEC)*, San Diego, CA, 2006, pp. 6.
- <sup>23</sup>Wright, Jerry, "Solar Arrays," *NASA Mission Page* [online], [https://www.nasa.gov/mission\\_pages/station/structure/elements/solar\\_arrays.html](https://www.nasa.gov/mission_pages/station/structure/elements/solar_arrays.html) [retrieved 20 January 2016].
- <sup>24</sup>Wenige, R., Schilbach, M., and Weider, P.F., "Power Storage for Small Satellites: Comparison of NiH2 and LiIon Batteries."
- <sup>25</sup>Jet Propulsion Laboratory, "Mars Exploration Rover Mission: The Mission," *Mars Exploration Rover Mission: The Mission*, [online], [http://mars.nasa.gov/mer/mission/spacecraft\\_edl\\_parachute.html](http://mars.nasa.gov/mer/mission/spacecraft_edl_parachute.html) [retrieved 17 Jan. 2016].
- <sup>26</sup>NASA Mars Exploration, "Balloons: Floating through Martian Air," *NASA Mars Exploration* [online], <http://mars.nasa.gov/programmissions/missions/missiontypes/balloons/> [retrieved 5 Oct. 2015].
- <sup>27</sup>Edquist, K., Berry, S., Kleb, B., Korzun, A., Dyakonov, A., Zarchi, K., Schauerhamer, G., Post, E., "Supersonic Retro-propulsion Technology Development in NASA's entry, Descent, and Landing Project," *National Aeronautics and Space Administration* [online], pp. 4, [https://solarsystem.nasa.gov/docs/02\\_Supersonic%20Retropropulsion%20Technology%20Development%20in%20NASA's%20Entry,%20Descent,%20and%20Landing%20Project\\_K.%20Edquist1.pdf](https://solarsystem.nasa.gov/docs/02_Supersonic%20Retropropulsion%20Technology%20Development%20in%20NASA's%20Entry,%20Descent,%20and%20Landing%20Project_K.%20Edquist1.pdf) [retrieved 7 April 2016].
- <sup>28</sup>NASA Science, "Strange but True: Curiosity's Sky Crane," [Online], [http://science.nasa.gov/science-news/science-at-nasa/2012/30jul\\_skycrane/](http://science.nasa.gov/science-news/science-at-nasa/2012/30jul_skycrane/) [retrieved 4 March 2016].
- <sup>29</sup>Braun, R. D., and Manning, R., "Mars exploration entry, descent and landing challenges," *2006 IEEE Aerospace Conference: Big Sky, Montana, 4-11 March 2006*, Piscataway, NJ: Institute of Electrical and Electronics Engineers, 2006.
- <sup>30</sup>Sengupta, A., Steltzner, A. "An Overview of the Mars Science Laboratory Parachute Decelerator System", [online], <http://ieeexplore.ieee.org/stamp/stamp.jsp?arnumber=4161343> [retrieved 13 March 2016]
- <sup>31</sup>Christensen, P., May, L., "ission Concept Study," *Planetary Science Decadal Survey MSR Lander Mission*, April 2010.



- <sup>32</sup>Way, D., Powell, R., Chen A., Steltzner A., Martin, A., Burkhart, P., Mendeck, G., "Mars Science Laboratory: Entry, Descent, and Landing System Performance", [online], <http://ntrs.nasa.gov/archive/nasa/casi.ntrs.nasa.gov/20090007730.pdf> [retrieved 2 April 2016].
- <sup>33</sup>Samareh, J., Komar, D. "Parametric Mass Modeling for Mars Entry, Descent and Landing System Analysis Study", [online], <http://ntrs.nasa.gov/archive/nasa/casi.ntrs.nasa.gov/20110005491.pdf> [retrieved 9 March 2016].
- <sup>34</sup>Del Corso, J., Cheatwood, F., Bruce, W., Hughes, S. "Advanced High-Temperature Flexible TPS for Inflatable Aerodynamic Decelerators," [online], <http://ntrs.nasa.gov/archive/nasa/casi.ntrs.nasa.gov/20110012051.pdf> [retrieved 14 March 2016].
- <sup>35</sup>Wolf, A. A., Graves, C., Powell, R., Johnson, W., "Systems for Pinpoint Landing at Mars," *Advances in the Astronautical Sciences*, published online 3 Feb. 2005; AAS 04-272.
- <sup>36</sup>Steinfeldt, B. A., Grant, M. J., Matz, D. A., Braun, R., "Guidance, Navigation, and Control System Performance Trades for Mars Pinpoint Landing," *Journal of Spacecraft and Rockets*, published online 12 Mar. 2010; Vol. 47, No. 1, 2010, pp 188-198; DOI: 10.2514/1.45779.
- <sup>37</sup>Tetzman, D. G., "Simulation and Optimization of Spacecraft Re-entry Trajectories," M. S. Dissertation, Minnesota Univ., Minneapolis, MN, 2010.
- <sup>38</sup>Wong, E. C., Singh, G., "Guidance and Control Design for Hazard Avoidance and Safe Landing on Mars," *Journal of Spacecraft and Rockets*, published online 30 Mar. 2006; Vol. 43, No. 2, 2006, pp 378-374.
- <sup>39</sup>Karlgard, C. D., Kutty, P., Schoenberger, M., Shidner, J., "Mars Science Laboratory Entry, Descent, and Landing Trajectory Atmosphere Reconstruction," AAS-13-307, February 2013.
- <sup>40</sup>Wolf, A., Tooley, J., Ploen, S., Gromov, K., Ivanov, M., and Acikmese, B., "Performance Trades for Mars Pinpoint Landing," 2006 IEEE Aerospace Conference, Paper 1661, IEEE Publications, Piscataway, NJ, March 2006. doi:10.1109/AERO.2006.1655793.
- <sup>41</sup>Hillje, E. R., "Entry Flight Aerodynamics From Apollo Mission AS-20," *NASA TN D-4185*, Oct. 1967.
- <sup>42</sup>Arya, R., and Shymija, M. Z., "The Advantages of Different Types of Propellants," *SlideShare* [online], <http://www.slideshare.net/aryamaru/the-advantages-of-different-types-of-propellants> [retrieved 10 Dec. 2016].
- <sup>43</sup>*Encyclopedia Astronautica* [online database], <http://www.astronautix.com/engines/index.htm> [retrieved 8 Feb. 2016].
- <sup>44</sup>Kirk, D., and London, A., "Comments on Rocket Scaling," Ventions, LCC, Florida Institute of Technology.
- <sup>45</sup>Venere, E., "Researchers cooking up new gelled rocket fuels," *Purdue University News* [online], 21 January, 2009, <http://www.purdue.edu/uns/x/2009a/090121HeisterGelled.html> [retrieved 8 Feb. 2016].
- <sup>46</sup>Chandler, A. A., Cantwell, B. J., Hubbard, G. S., and Karabeyoglu, A., "Feasibility of a single port Hybrid Propulsion system for a Mars Ascent Vehicle," *Acta Astronautica* 1066-1072, Feb. 2011.
- <sup>47</sup>Arnold, D. M., "Formulation and Characterization of Paraffin-Based Solid Fuels Containing Swirl Inducing Grain Geometry And/Or Energetic Additives," *A Thesis in Mechanical Engineering*, The Pennsylvania State University, May 2014.
- <sup>48</sup>Story, G., "Genetic Algorithm Optimization of a Cost Competitive Hybrid Rocket Booster," NASA MSFC, Huntsville, AL.
- <sup>49</sup>Geyzel, D., Cantwell, B., Karabeyoglu, A., Micheletti, D., and Stevens, J., "High Performance Hybrid Upper Stage Motor", AIAA.
- <sup>50</sup>Cantwell, B. J., Chandler, A. A., Hubbard, G. S., and Karabeyoglu, A., "A Two-Stage, Single Port Hybrid Propulsion System for a Mars Ascent Vehicle," *46th AIAA/ASME/SAE/ASEE Joint Propulsion Conference & Exhibit*, AIAA, Nashville, TN, July 2010.
- <sup>51</sup>Beckwith, R., Stoll, A., Tybor, F., Waxman, B. S., and Zimmerman, J., "Paraffin and Nitrous Oxide Hybrid Rocket as a Mars Ascent Vehicle Demonstrator," *AIAA Space 2010 Conference & Exposition*, AIAA 2010-8840, Anaheim, CA, Aug.t 2010.
- <sup>52</sup>Hubbard, G. S., Cantwell, B. J., Chandler A. A., Goldstein, B., Karabeyoglu M. A., and Reeve, R., "A Storable, Hybrid Mars Ascent Vehicle Technology Demonstrator for the 2020 Launch Opportunity," *Concepts and Approaches for Mars Exploration*, 2012.
- <sup>53</sup>Chelaru, A., Chelaru, T., and Enache, V., "Reaction Control System using Hybrid Micro-Thrusters, Theoretical and Experimental Results," *IEEE Xplore*.
- <sup>54</sup>"Mars Ascent Vehicle: In-Space Propulsion Technology Program," *NASA Facts*, MAV-2012-3-12-GRC, NASA Glenn Research Center, Cleveland, OH.
- <sup>55</sup>Sengupta, A., Trinidad, M. A., and Zabrensky, E., "Mars Ascent Vehicle System Studies and Baseline Conceptual Design," *IEEE*, 2012.
- <sup>56</sup>Burg, B. R., Dubowsky, S., Lienhard, J. H. V., and Poulikakos, D., "Thermal Control Architecture for a Planetary and Lunar Surface Exploration Micro-Robot," *Laboratory for Thermodynamics in Emerging Technologies*, Zurich, Switzerland.
- <sup>57</sup>Birur, G. C., Pauken, M. T., and Novak, K. S., "Thermal Control of Mars Rovers and Landers Using Mini Loop Heat Pipes," *Jet Propulsion Laboratory, California Institute of Technology*, Pasadena, California.
- <sup>58</sup>Robinson, G., "ARTICLE IX OF THE OUTER SPACE TREATY: Extraterrestrial Back Contamination, the U.S. Constitution, and the Politics of U.S. Regulatory Authority," *Space Law* [online], <http://www.spacelaw.olemiss.edu/events/pdfs/2010/galloway-robinson-paper-2010.pdf> [retrieved Nov. 2015].
- <sup>59</sup>Ammann, W., Barros, J., Bennett, A., Bridges, J., Fragola, J., Kerrest, A., ... & Salminen, M. (2012). "Mars Sample Return backward contamination strategic advice and requirements" - Report from the ESF-ESSC Study Group on MSR Planetary Protection Requirements.
- <sup>60</sup>Atlas, R., "Planetary Protection Mars Sample Return Receiving Facility," *Lunar and Planetary Institute* [online], <http://www.lpi.usra.edu/pss/presentations/200803/04-atlas-ppsonmsr.pdf> [retrieved 24 Nov. 2015].
- <sup>61</sup>Akin, D., "Applications of Ultra-Low Ballistic Coefficient Entry Vehicles to Existing and Future Space Missions," *SpaceOps 2010 Conference - Delivering on the Dream - Hosted by NASA Marshall Space Flight Center and Organized by AIAA*, Apr. 2010.

- <sup>62</sup>"Stardust Sample Return - Press Kit," *NASA JPL* [online] [http://www.jpl.nasa.gov/news/press\\_kits/stardust-return.pdf](http://www.jpl.nasa.gov/news/press_kits/stardust-return.pdf) [retrieved 8 Feb. 2016].
- <sup>63</sup>Garner, R., "How to Protect Astronauts from Space Radiation on Mars", *NASA* [online], <http://www.nasa.gov/feature/goddard/real-martians-how-to-protect-astronauts-from-space-radiation-on-mars> [retrieved 20 Jan. 2016].
- <sup>64</sup>Thibeault, S., Fay, C., Lowther, S., Earle, K., Sauti, G., Ho Kan, J., Park, C., "Radiation Shielding Materials Containing Hydrogen, Boron, and Nitrogen: Systematic Computational and Experimental Study - Phase I", *NASA* [online], [https://www.nasa.gov/pdf/716082main\\_Thibeault\\_2011\\_PhI\\_Radiation\\_Protection.pdf](https://www.nasa.gov/pdf/716082main_Thibeault_2011_PhI_Radiation_Protection.pdf) [retrieved 21 Feb. 2016].
- <sup>65</sup>NASA, "NASA Technology Roadmaps TA 6: Human Health, Life Support, and Habitation", *NASA* [online], [http://www.nasa.gov/sites/default/files/atoms/files/2015\\_nasa\\_technology\\_roadmaps\\_ta\\_6\\_human\\_health\\_life\\_support\\_habitation\\_final.pdf](http://www.nasa.gov/sites/default/files/atoms/files/2015_nasa_technology_roadmaps_ta_6_human_health_life_support_habitation_final.pdf) [retrieved 12 Feb. 2016].
- <sup>66</sup>"Ka vs. Ku - An Unbiased Review," *Skyware Technologies* [online], <http://www.skywaretechnologies.com/news/item/84-ka-vs-ku-an-unbiased-review> [retrieved 10 Feb. 2016].
- <sup>67</sup>Harlow, P., "Commercial X-band: In the ring with Ku- and Ka-Band," *XSTAR* [online], <http://xtar.com/2013/02/07/commercial-x-band-in-the-ring-with-ku-and-ka-band/> [retrieved 17 Feb. 2016].
- <sup>68</sup>"Space Communications with Mars," *Astrosurf* [online], <http://www.astrosurf.com/luxorion/qs1-mars-communication3.htm> [retrieved 10 Feb. 2016].
- <sup>69</sup>"Satellites - Communications: Dish Antennas," *Galactics* [online], <http://satellites.spacesim.org/english/anatomy/comm/dish.html> [retrieved 9 Feb. 2016].
- <sup>70</sup>"Mechanisms - Mars Reconnaissance Orbiter," *NASA* [online], <http://mars.nasa.gov/mro/mission/spacecraft/parts/mechanisms/> [retrieved 4 Feb. 2016].
- <sup>71</sup>"Antennas - Mars Reconnaissance Orbiter," *NASA* [online], <http://mars.nasa.gov/mro/mission/spacecraft/parts/antennas/> [retrieved 16 Feb. 2016].
- <sup>72</sup>*Space Launch Report* [online], [www.spacelaunchreport.com/library.html#lvddata](http://www.spacelaunchreport.com/library.html#lvddata) [retrieved 14 April 2016]
- <sup>73</sup>Fehse, W., "Sensors for Automated Rendezvous Navigation," *Automate Rendezvous and docking of Spacecraft Vol. 16*, New York, NY, 2003, pp 218-282.
- <sup>74</sup>Barbee B. W. B, Carpenter J. R., Heatwole S., Markley F. L., Moreau M., Naasz B. J., Van Eepoel J., "A Guidance and Navigation Strategy for Rendezvous and Proximity Operations with a Noncooperative Spacecraft in Geosynchronous Orbit," *The Journal of the Astronautical Sciences*, published online 15 Sept. 2011; Vol. 58, No. 3, 2011, pp 389-408.
- <sup>75</sup>Woffinden, D. C., "Angles-Only Navigation for Autonomous Rendezvous," Ph.D. Dissertation, Mechanical Engineering Department, Utah Univ., Logan, UT, 2008.
- <sup>76</sup>Balmanno, W. F., Whiddon, W. B., Anderson, R. L., "Mars Sample Return Mission Studies Leading to a Reduced-Risk Dual-Lander Mission Using Solar Electric Propulsion," TRW, Inc., Redondo Beach, CA, May 2001.
- <sup>77</sup>Stuit, T. D., "Designing the STS-134 Re-Rendezvous: A Preparation for Future Crewed Rendezvous Missions," *AIAA Space 2011 Conference and Exposition*, American Inst. of Aeronautics and Astronautics, Long Beach, CA, 2011, pp. 1-29.
- <sup>78</sup>Larson, W. J., and Wertz, J. R., "Cost Modeling," *Space Mission Analysis and Design*, 3rd ed., El Segundo, CA, 1999, pp. 783-788.
- <sup>79</sup>"Advanced Missions Cost Model," *Federation of American Scientists* [online], <http://fas.org/news/reference/calc/AMCM.htm> [retrieved 16 April 2016].
- <sup>80</sup>"Mars Sample Return Implementation Discussions," *NASA JPL* [online], <http://www.spacepolicyonline.com/images/stories/PSDS%20Mars%20Li-MSR.pdf> [retrieved 17 April 2016].
- <sup>81</sup>Mattingly, R., "Mission Concept Study: Planetary Science Decadal Survey MSR Lander Mission," *NASA JPL*, April 2010.
- <sup>82</sup>Mustard, J., "MEPAG Report to the Planetary Science Subcommittee," *Mars Exploration Program Analysis Group (MEPAG)* [online], <http://www.lpi.usra.edu/pss/presentations/200803/07-Mustard-MEPAG.pdf> [retrieved 17 April 2016].

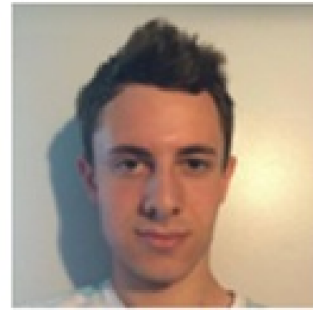
## Team Members



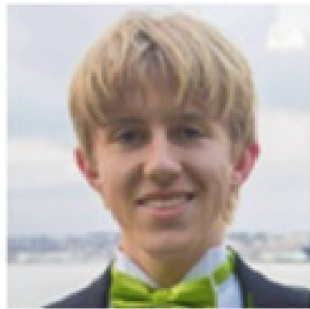
**Archit Arora**  
**Orbitals Lead**  
**677258**



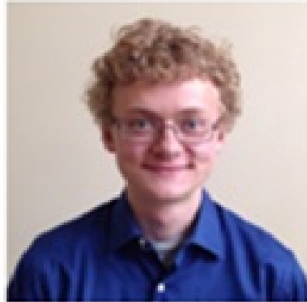
**Courtney Best**  
**Mars Ascent Lead**  
**513756**



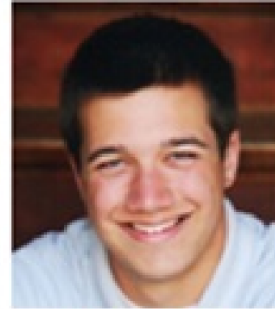
**Liam Durbin**  
**Earth Recovery Lead**  
**607359**



**Robert Groome**  
**CAD Lead**  
**464631**



**Duncan Harris**  
**Mars Descent Lead**  
**644965**



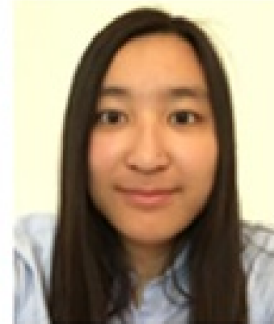
**Henry Heim**  
**Structures Lead**  
**606462**



**Thomas Keane**  
**Navigation Lead**  
**514978**



**Eric Miller**  
**Power Lead**  
**474001**



**Annie Ping**  
**Transfer Vehicle Lead**  
**513786**



**Alexandra Wyatt**  
**Communications Lead**  
**676817**